



## Characteristics and process controls of statistical flood moments in Europe – a data based analysis

David Lun<sup>1</sup>, Alberto Viglione<sup>2</sup>, Miriam Bertola<sup>1</sup>, Jürgen Komma<sup>1</sup>, Juraj Parajka<sup>1</sup>, Peter Valent<sup>1,3</sup>, Günter Blöschl<sup>1</sup>

- 5 <sup>1</sup>Institute of Hydraulic Engineering and Water Resources Management, Vienna University of Technology, Vienna, Austria  
<sup>2</sup>Department of Environment, Land and Infrastructure Engineering, Politecnico di Torino, Turin, Italy  
<sup>3</sup>Department of Land and Water Resources Management, Faculty of Civil Engineering, Slovak University of Technology, Bratislava, Slovakia
- 10 *Correspondence to:* David Lun (lun@hydro.tuwien.ac.at)

**Abstract.** This paper analyses the spatial patterns and process controls of the mean annual flood (MAF), coefficient of variation (CV) and skewness (CS) of flood discharges in Europe. The data consist of maximum annual flood discharge series observed in 2370 catchments in Europe covering the period 1960-2010. On average, in Europe, the estimated moments MAF, CV and CS are  $0.17 \text{ m}^3 \text{ s}^{-1} \text{ km}^{-2}$ , 0.52 and 1.28, respectively.

The results indicate that MAF is largest along the Atlantic coast, the high rainfall areas of the Mediterranean coast and in the mountain ranges of Europe, while it is smallest in the sheltered parts of the East European plain. CV is largest in Southern and Eastern Europe, while it is smallest in the regions of strong Atlantic influence. The pattern of CS is similar to that of CV, albeit a little more erratic. In the Mediterranean, MAF, CV and CS decrease strongly with catchment area suggesting that floods in small catchments are relatively very large, while in Eastern Europe the dependence is much weaker.

The Process controls on the flood moments in five hydroclimatic regions are identified by correlation and multiple linear regression analyses with a range of covariates. Precipitation-related variables are found to be the main controls of the spatial patterns of MAF in most of Europe except for the regions with snow influence where air temperature is more important. Catchment area is another relevant variable. Aridity is by far the most important control of the spatial pattern of CV in all of Europe. Precipitation-related variables are relevant in Southern Europe. Overall, the findings suggest that, at the continental scale, climate variables dominate over land surface characteristics, such as land use and soil type, in controlling the spatial patterns of flood moments.

Finally, the estimation accuracy of the multiple linear regression model for estimating flood moments in ungauged basins is evaluated as a baseline for more accurate local studies.

### 1. Introduction

Understanding the spatial distribution of statistical flood characteristics is important from both practical and theoretical perspectives, assisting in estimating design floods in gauged and ungauged catchments, and shedding light on the regional processes of flood generation from a probabilistic perspective (Rosbjerg et al., 2013).



Much research has been conducted on identifying process variables and mechanisms controlling the magnitudes of flood characteristics. Catchment area usually is the main control on the specific mean annual flood (MAF) (Rosbjerg et al., 2013). This is because a large basin is less likely to be fully covered by a thunderstorm than a small basin which tends to reduce the variance of extreme catchment-average precipitation and thus the MAF (Viglione et al., 2010a, b). Additionally, there is a space-time effect. Event-scale catchment response times tend to increase with area (Gaál et al. 2012), which leads to a greater attenuation of the flood peaks. The effect of catchment area on the CV (the ratio of standard deviation and annual means) tends to be more complex. For example, Smith (1992), based on data in the Appalachian region, found an increase in CV with catchment area up to about 100 km<sup>2</sup>, and subsequently a decrease, which he explained by the spatial organisation of precipitation and downstream changes in the floodplain system. Blöschl and Sivapalan (1997) suggested that space-time scale interactions may be the main reason of the scale dependence, while Merz and Blöschl (2003) noted that the strength of the dependence of CV on area will differ between regions of different prevailing flood generation types such as synoptic floods and snowmelt driven floods. Based on an analysis of flood data in Slovakia, Austria and Italy, Salinas et al. (2014b) found both CV and CS to decrease with catchment area which they interpreted as the result of aggregation effects of the spatial heterogeneity of rainfall and the interaction between the spatial and temporal scales of rainfall and catchment size.

Runoff generation and thus flood moments are also controlled by soil characteristics, geology and land-use. Most of the knowledge on these effects comes from simulation studies. For example, Gioia et al. (2012) demonstrated that infiltration and soil storage strongly affect the flood moments, and Brath et al. (2006) performed a similar analysis for the case of land use. The role of these variables can to some extent be inferred from their use as covariates in flood frequency regionalisation (see, e.g. Zaman et al., 2012; Rosbjerg et al., 2013; Miller and Brewer, 2018). However, the type of soil, geology and land-use data available at the regional scale is often not consistent with the level of detail required for quantifying runoff generation processes, and therefore correlations with flood characteristics tend to be low (Weingartner et al., 2003).

Another important control is climate. Mechanistically, one would expect extreme precipitation to represent flood characteristics as it is usually the main driver at the event scale (Viglione et al., 2009). However, many studies have shown that mean annual precipitation (MAP) is a better predictor of MAF (e.g. Madsen et al., 1997; Reed et al., 1999; Merz and Blöschl, 2009) for which a number of reasons have been suggested: MAP is usually highly correlated to event precipitation; MAP is an important control of antecedent soil moisture on a seasonal scale (e.g. Grillakis et al., 2016); and climate, vegetation, soils and land forms may co-evolve with MAP, thus exerting a longer term influence (Gaál et al., 2012, Perdigão and Blöschl, 2014). Based on data from around the world, Farquharson et al. (1992) found CV to increase with aridity (the ratio of potential evaporation and MAP), and Merz and Blöschl (2009) found potential evaporation to be an excellent predictor of MAF and CV in the lowlands of Austria which they interpreted in terms of the increasing non-linearity of the rainfall-runoff process with aridity. Iacobellis et al. (2002), found that CV behaviour is controlled mainly by the long-term climate and the abstraction characteristics at the catchment scale. While a decrease in CV with the area is attributed to catchments where the infiltration excess (Horton type) mechanism dominates, as in arid and impermeable basins, an increase of CV with the catchment size is attributed to humid and vegetated catchments with dominant saturation excess runoff generation.



75 The climate controls, including rainfall, soil moisture and snowmelt are usually subject to strong seasonality. An  
analysis of the seasonality of floods (Bayliss and Jones, 1993; Merz and Blöschl, 2003) has therefore been an  
efficient way to shed light on the interaction of these processes. For example, based on a seasonality of 4262  
catchments in Europe, Blöschl et al. (2017) and Hall et al. (2018) identified extreme winter precipitation in  
northwestern Europe, snowmelt in northeastern and eastern Europe and summer precipitation and snowmelt in  
80 the Alpine regions of Europe to be important flood drivers. Using their data set, Berghuijs et al. (2019) found  
soil moisture excess to explain flood seasonality better than other variables such as extreme precipitation,  
particularly in the western part of Europe, in line with a similar study in the United States (Berghuijs et al.,  
2016).

While substantial understanding of regional flood controls has been achieved in the past, few studies have  
85 analysed large, consistent data sets of flood discharges in terms of their statistical moments. Large data sets  
provide the opportunity of obtaining more robust and generalisable findings than studies containing a smaller  
number of catchments. The aim of this paper is therefore to identify the continental scale patterns of flood  
moments and their controls across Europe. We use a data set of flood discharges of 2370 catchments across  
Europe for the period 1960-2010 and apply correlation and regression analyses to identify climatic and  
90 catchment process controls on the moments.

## 2. Data and Methodology

### 2.1 Data

This study uses the data set of European flood discharges of Blöschl, Hall et al. (2019), which can be found in  
95 their supplementary material. It consists of 2370 annual maximum peak discharge series from 33 countries.  
Catchment areas range from 5 to 100000 km<sup>2</sup>, with a median of 383 km<sup>2</sup>. The observation period is 1960 to  
2010, and record lengths range from 30 to 51 years with a median of 51 years.

In order to analyse process controls, a range of catchment attributes and climatic indicators are used. In addition  
to catchment area, we used catchment-averaged climate indicators, including long-term mean annual  
100 precipitation (MAP), long-term mean potential evaporation (PET) and the aridity index, PET/MAP. Extreme  
precipitation is quantified by the daily rainfall rate that is not exceeded in 95% of the days, and the long-term  
mean of the maximum 2-day precipitation of each year. As a proxy for snowmelt we used the mean air  
temperature in spring (MAM) and winter (DJF). Soil moisture was taken from the CPC Soil moisture database,  
which contains model-calculated soil moisture values. We used the mean of the annual maximum monthly  
105 values over the observation period. Topographical indicators include the mean catchment elevation and the mean  
topographical slope of each catchment. Land use was quantified by the percentage of land use classes. Soil  
characteristics were quantified in terms of soil texture classified into five categories. The data used are  
summarised in Table 1.

110 Table 1: Data used in this study including quantiles of the variables and source information. Sources:

<sup>1</sup>Data base on European floods: [https://github.com/tuwhydro/europe\\_floods](https://github.com/tuwhydro/europe_floods)

<sup>2</sup>CCM River and Catchment Database. Vogt et al., 2017. <https://data.europa.eu/>

<sup>3</sup>E-OBS gridded dataset (v18.0e), 0.1 deg. Comes et al., 2018. <https://www.ecad.eu/>



115 <sup>4</sup>Global Aridity Index and Potential Evapo-Transpiration (ET0) Climate Database V2. Trabucco and Zomer, 2019  
[https://figshare.com/articles/Global\\_Aridity\\_Index\\_and\\_Potential\\_Evapotranspiration\\_ET0\\_Climate\\_Database\\_v2/7504448/3](https://figshare.com/articles/Global_Aridity_Index_and_Potential_Evapotranspiration_ET0_Climate_Database_v2/7504448/3)

<sup>5</sup>CPC Soil Moisture (V2), NOAA Climate Prediction Center. Fan and Dool, 2004. <https://www.cpc.ncep.noaa.gov/>

<sup>6</sup>Global Multi-resolution Terrain Elevation Data GMTED2010, 7.5 arc-seconds. <https://www.usgs.gov/>

<sup>7</sup>Corine Land Cover (CLC) 2000, Version 20b2, <https://land.copernicus.eu/>

120 <sup>8</sup>European Soil DataBase (ESDB), Soil Geographical DataBase (SGDB), TEXT\_SRF\_DOM, 10x10km. Panagos et al., 2012.  
<https://esdac.jrc.ec.europa.eu>

| Variable group  | Symbol           | Data Description  | Units   | 25 / 50 / 75% quantiles | Source  |
|-----------------|------------------|---|---|-------------------------|---|
| Flood Moments   | MAF              | Mean annual specific flood  | m <sup>3</sup> s <sup>-1</sup>                  | 0.06/0.11/0.22          | Data base on European floods <sup>1</sup>   |
|                 | MAF <sub>α</sub> | Mean annual specific flood normalized to catchment area of α = 100km <sup>2</sup>                               | m <sup>3</sup> s <sup>-1</sup> km <sup>-2</sup> | 0.08/0.16/0.28          | Data base on European floods <sup>1</sup>   |
|                 | CV               | Coefficient of variation of annual maximum flood peaks  | -   | 0.36/0.46/0.61          | Data base on European floods <sup>1</sup>   |
|                 | CS               | Coefficient of skewness of annual maximum flood peaks   | -   | 0.62/1.09/1.69          | Data base on European floods <sup>1</sup>   |
| Catchment Area  | A                | Catchment area  | km <sup>2</sup>                                 | 135.90/382.80/1264.80   | CCM River and Catchment Database <sup>2</sup>   |
| Precipitation   | MAP              | Long-term mean annual precipitation   | mm yr <sup>-1</sup>                             | 621.28/798.69/1057.76   | EOBS <sup>3</sup>   |
|                 | P95              | Daily precipitation rate, that is higher than what is observed on 95% of days in the observed period            | mm d <sup>-1</sup>                              | 8.40/10.54/13.45        | EOBS <sup>3</sup>   |
|                 | Pmax             | Mean of maximum of 2-day precipitation of each year   | mm d <sup>-1</sup>                              | 18.00/22.45/28.51       | EOBS <sup>3</sup>   |
| Air temperature | Tspr             | Mean daily temperature in MAM (Celsius)   | °C  | 5.03/7.15/8.42          | EOBS <sup>3</sup>   |
|                 | Twin             | Mean daily temperature in DJF (Celsius)   | °C  | -3.35/-1.16/1.05        | EOBS <sup>3</sup>   |
| Soil moisture   | SM               | Mean of annual maximum monthly soil moisture  | mm  | 368.38/424.93/507.20    | CPC Soil Moisture (V2) <sup>5</sup>   |
| Evaporation     | PET              | Long-term mean potential evaporation  | mm yr <sup>-1</sup>                             | 749.02/817.73/897.98    | Global Aridity Index and Potential Evapo-Transpiration (ET0) Climate Database V2 <sup>4</sup> |
| Aridity         | AI               | Aridity index (PET/MAP)   | unitless  | 0.72/1.00/1.25          | Global Aridity Index and Potential Evapo-Transpiration (ET0) Climate Database V2 <sup>4</sup> |
| Topography      | Elev             | Mean catchment elevations   | m a.s.l.  | 199.04/472.58/833.12    | GMTED2010 <sup>6</sup>  |
|                 | Slope            | Mean topographic slope (mean of tangent of angle of slope)  | unitless  | 0.03/0.08/0.18          | GMTED2010 <sup>6</sup>  |
| Land use        | LUF              | Fraction of catchment area covered by forest and seminatural areas  | %   | 31.66/54.59/79.62       | CORINE <sup>7</sup>   |
|                 | LUW              | Fraction of catchment area covered by water bodies  | %   | 0/0.05/0.57             | CORINE <sup>7</sup>   |
| Soils           | Stex             | Dominant surface textural class of the STU (Soil Typological Unit), mean value of categories (1=coarse, 5=fine) | class   | 1.77/2.00/2.25          | ESDB <sup>8</sup>   |



## 2.2 Hydroclimatic regions

For the statistical analyses, Europe was subdivided into five regions based on a particularization of the eleven biogeographic regions of Roekaerts (2002) and guided by the flood seasonalities of Blöschl et al. (2017) and Hall et al. (2018). In the Northeastern region floods are mainly due to snowmelt during spring and early summer. The Atlantic region is characterised by mild, wet winters and cool, humid summers; floods mainly occur in winter. The Central-Eastern region has a continental climate with cold winters and warm summers and floods mainly occur in spring with snow melt contributions. The Alpine region involves the Alps and the Carpathians where floods mainly occur in summer due to summer storms and/or snow melt. The Mediterranean region is characterised by hot dry summers and mild wet winters; floods occur in autumn and winter. For simplicity, each catchment was allocated to one of the regions according to the location of its stream gauge.

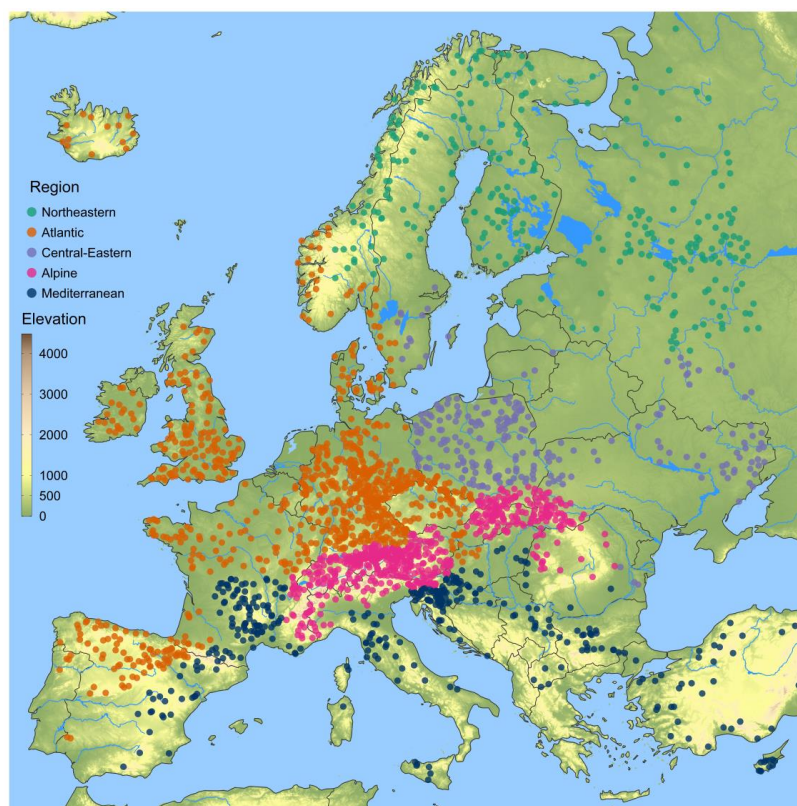


Figure 1: Location of the 2370 hydrometric stations analyzed. Colours of dots indicate five hydro-climatic regions (Northeastern, Atlantic, Central-Eastern, Alpine, Mediterranean). Background colour is elevation (m a.s.l.).

135

## 2.3 Analysis method

The statistical flood moments, the specific mean annual flood (MAF), the coefficient of variation (CV) and the coefficient of skewness (CS), were estimated from the annual maximum peak discharges series by:

$$MAF = \frac{1}{n} \sum_{i=1}^n Q_i \quad (1)$$



$$140 \quad S^2 = \frac{1}{n-1} \sum_{i=1}^n (Q_i - MAF)^2 \quad (2)$$

$$CV = \frac{S}{MAF} \quad (3)$$

$$CS = \frac{n \sum_{i=1}^n (Q_i - MAF)^3}{(n-1)(n-2)S^3} \quad (4)$$

where  $Q_i$  is the annual maximum peak discharge of a record in year  $i$ , divided by the catchment area. Estimation uncertainty of the statistical flood moments decreases with record length and increases with the moment order.

145 While the estimation uncertainty of the mean is small, the uncertainty of CS can be substantial. For a record length of 50 years and a series with the average estimated moments of the entire dataset ( $MAF=0.17 \text{ m}^3 \text{ s}^{-1} \text{ km}^{-2}$ ,  $CV=0.52$ ,  $CS=1.28$ ), the standard error of the CS estimate is  $\sigma_{CS}=0.56$ , which is about half of the underlying true moment (assuming a GEV-distribution as the data-generating process). The estimation uncertainties need to be accounted for when interpreting the process controls on the flood moments. Since the specific mean annual  
 150 flood is often strongly controlled by catchment area which may mask other controls that vary regionally, we additionally considered the specific mean annual flood,  $MAF_\alpha$ , normalised to a catchment area of  $\alpha=100 \text{ km}^2$

$$MAF_\alpha = MAF \alpha^{-\beta_{MAF}} \quad (5)$$

$MAF_\alpha$  and  $\beta_{MAF}$  were found by ordinary least squares regression.

In a first step we estimated what fraction of the spatial variability of the estimated flood moments can be  
 155 explained by subdividing Europe into five regions (Figure 1), using a simple one-way analysis of variance (ANOVA). This can be interpreted as a simple regression model, where the dependent variables are the estimated flood moments and the only explanatory variables are indicators corresponding to the regional partition. The coefficient of determination of this model corresponds to the fraction of variance explained by the partition over the total variance in estimates of the flood moments.

160 In a second step we evaluated the role of catchment area, since it is almost always the main control on the mean annual flood and reflects the aggregation behaviour of the floods and its controls. Specifically we estimated the dependence of MAF, CV and CS on catchment area in a double logarithmic relationship from Eq. (5) and analogous equations for CV and CS.

In a third step we conducted a seasonality analysis to assist in the process interpretations. We represented the  
 165 date of occurrence,  $D$ , of the maximum annual flood as a number from 1 to 365 in polar coordinates on a unit circle with angle  $\theta = D \frac{2\pi}{365}$ . For a flood series, the direction  $\bar{\theta}$  of the average vector from the origin indicates the mean date of occurrence of the flood events around the year. The length of the vector from the origin is a measure of the variability of the date of occurrence, ranging from 0 (uniformly distributed across the year) to 1 (all events on the same day).

170 In a fourth step we analysed the effects of individual hydro-climatic controls on the spatial distribution of the flood moments. We used the attributes of Table 1 for the analysis. To assist in the interpretation we first evaluated the Spearman rank correlation coefficients between the attributes, followed by an analysis of the Spearman rank correlation coefficients between the flood moments and the attributes. We used Spearman's rank correlation coefficients, as non-linear associations between variables are possible. The corresponding



175 significance tests for the estimates of Spearman's rho are employed with the assumption of an asymptotic t-distribution under the Null Hypotheses (Gibbons and Chakraborti, 2010). The correlations were evaluated for all of Europe and the five regions separately.

In a fifth step we evaluated the effect of multiple controls on the flood moments. Multiple linear regression models were fitted to the estimated moments. The emphasis was on obtaining parsimonious models, therefore  
180 the number of selected variables for a regression equation was limited to four. The variables were log-transformed if feasible. The attributes were selected according to a stepwise selection procedure (Weisberg, 2005). The criterion for model comparison was Mallows' Cp

$$C_p = \frac{RSS_p}{\hat{\sigma}^2} + 2p - n \quad (6)$$

where  $p$  refers to the number of coefficients in the current model including the intercept and  $n$  to the number of  
185 observations.  $RSS_p$  is the residual sum of squares of the model being considered with  $p$  covariates and  $\hat{\sigma}^2$  is the residual error variance of the model including all possible covariates. For the comparisons of information criteria such as  $C_p$ , a complete set of observations is required, therefore 22 catchments, where some observations of covariates were not available, were excluded from this part of the analysis.

In order to assess which of the covariates in each regression provided the most explanatory power, a dominance  
190 analysis was conducted (Azen and Budescu, 2003). We used the measure for general dominance, which summarizes the average increase in the measure for the goodness of fit, when a given covariate is included in a regression model, for all possible model subsets for a fixed set of predictors. The sum of all measures for general dominance of each variable results in the  $R^2$  of the full regression. The general dominance measure (average contributions) provides a ranking of the variables in terms of contributions to the fit of the models ( $R^2$ ).  
195 However, this is only valid in the context of the model and the selected variables. These contributions can and most likely will change when variables are added to or subtracted from the regressions. To facilitate the interpretation of results, in section 3.5 we present the general dominance measure of individual covariates, divided by the  $R^2$  of the regression, and refer to this as the normalised general dominance measure. This does not affect the ranking of the variables.

200 In a sixth step the predictive accuracy of the fitted regression models was assessed in a leave-one-out cross-validation. The errors are evaluated on the scale of the data, instead of the scale of the regression models (i.e. log scale) and normalized, e.g. in the case of the MAF:

$$ANE_{MAF} = \left| \frac{\widehat{MAF} - MAF}{MAF} \right| \quad (7)$$

205 ANE stands for absolute normalized error.  $\widehat{MAF}$  are the predictions of the regression models and MAF are the at-site estimates. The analogous holds for CV.

In addition, ordinary kriging is used for interpolating the at-site estimates of flood moments (Cressie, 1993) and the interpolated values are contrasted with the predictions of regional regression models.



### 3. Results

#### 210 3.1 Characteristics of flood moments

Table 2 shows the characteristics of the estimated flood moments for the five hydroclimatic regions and the entire data set. On average over the entire data set, the mean specific annual flood is  $0.17 \text{ m}^3 \text{ s}^{-1} \text{ km}^{-2}$ , while the mean specific annual flood normalised to a catchment area of  $100 \text{ km}^2$  ( $\text{MAF}_a$ ) is  $0.21 \text{ m}^3 \text{ s}^{-1} \text{ km}^{-2}$ . The latter is somewhat larger, as  $100 \text{ km}^2$  is smaller than the median catchment size of  $383 \text{ km}^2$ . On average over the entire

215 data set, the CV and CS are 0.52 and 1.28, respectively. The regions differ in terms of the moments. The largest average  $\text{MAF}_a$  occurs in the Alpine region and in the Mediterranean ( $0.30 \text{ m}^3 \text{ s}^{-1} \text{ km}^{-2}$ ). The smallest average  $\text{MAF}_a$  ( $0.05 \text{ m}^3 \text{ s}^{-1} \text{ km}^{-2}$ ) occurs in the Central Eastern region, but this is also the region where the average CV and CS are largest (0.69 and 1.59, respectively). On the other hand, the Northeastern region has the smallest average CV and CS (0.39 and 0.82, respectively).

220 The coefficient of determination  $R^2$  of the one-way ANOVA is an indicator of how much of the spatial variability is explained by the partitioning into the five regions. The partitioning explains 17% of the spatial variance of  $\text{MAF}_a$ , but only 9% and 5% of the spatial variance of CV, CS, respectively. This means that the spatial variability within the regions of CV and CS is similar to that over all of Europe. Part of that variability may be sampling uncertainty, but Figure 2 indicates that, at least for  $\text{MAF}_a$  and CV, there are clear spatial

225 patterns which, however, are not aligned with the regions. As the regions have not been chosen to reflect flood magnitudes but rather hydro-climatic processes this is not surprising.

The largest  $\text{MAF}_a$  occur in the Alps, the Appenines, the Carpathian Flysch Belt, adjacent to the Ligurian and Adriatic Seas, the Languedoc, and the western coasts of Great Britain and Norway, which are all high rainfall areas. The lowest  $\text{MAF}_a$  occurs in the North and East European Plains, Dnieper Lowland, Finish Lakeland and

230 southern Sweden and south-eastern England (Fig. 2c).  $\text{MAF}_a$  exhibits slightly more homogeneous spatial patterns than MAF as the effect of catchment size has been removed. The spatial distribution of CV is, to some degree, a mirror image of that of  $\text{MAF}_a$ , as CV and  $\text{MAF}_a$  are negatively correlated with a Spearman correlation coefficient of  $r=-0.12$  ( $-0.06$  for CV vs MAF). However, there are deviations from this general pattern. Along the Mediterranean coast between Genua and Valencia CVs are rather large even though  $\text{MAF}_a$  are large too. The

235 spatial distribution of CS is less apparent, as roughly half the spatial variability is likely attributable to sampling variability (the standard error of the CS estimate for average parameters is  $\sigma_{CS} = 0.56$ ). However, there seems to exist a general pattern of larger than average CS along the Mediterranean coast and the mountainous areas of Europe, and smaller than average CS in Scandinavia and northern Russia. There is a strong positive Spearman correlation between CS and CV ( $r=0.63$ ) which points towards non-linear runoff generation processes affecting

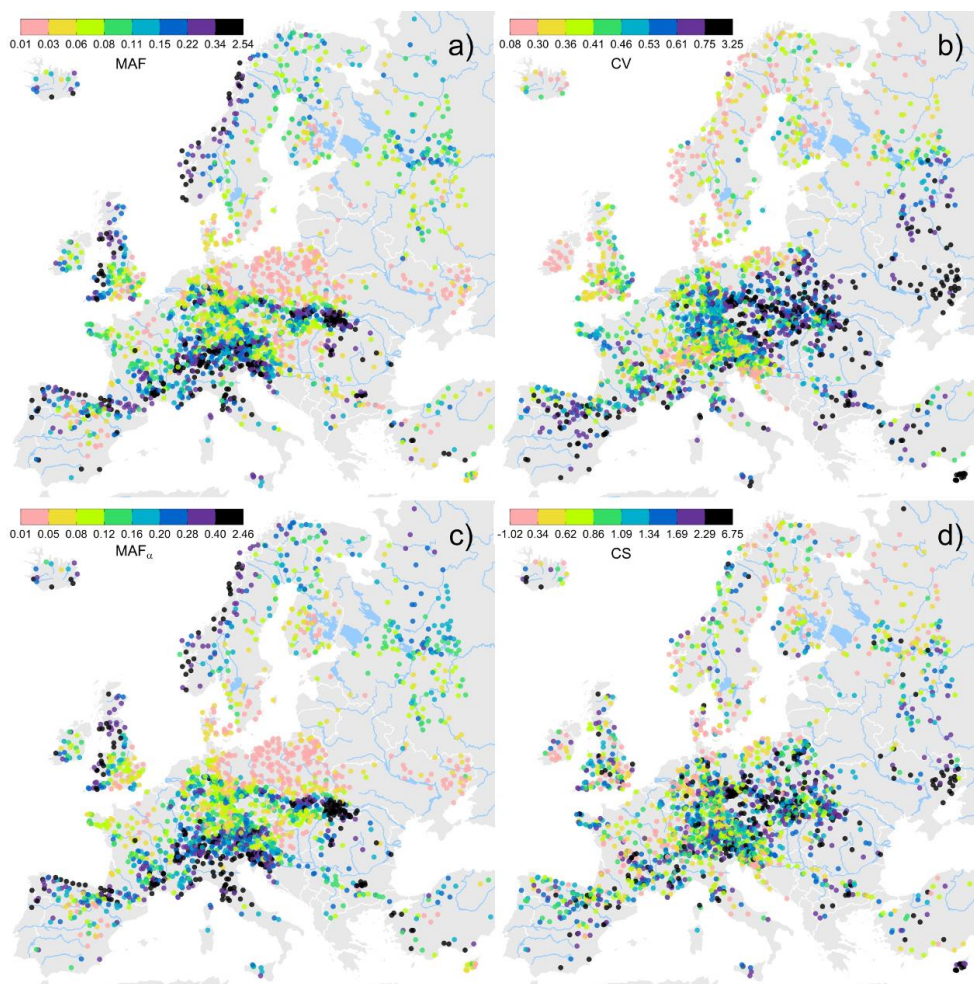
240 both CS and CV (Rogger et al., 2013), although, again the correlation may be partly due to the sampling variability resulting in correlations between the estimators of CV and CS (see chapter 10 in Kendall and Stuart, 1969).

245 Table 2: Regional mean (m) and regional coefficient of variation (cv) of the mean annual specific flood (MAF, ( $\text{m}^3 \text{ s}^{-1} \text{ km}^{-2}$ )), mean annual specific flood normalised to catchment area of  $100 \text{ km}^2$  ( $\text{MAF}_a$ , ( $\text{m}^3 \text{ s}^{-1} \text{ km}^{-2}$ )), coefficient of variation (CV) and coefficient of skewness (CS) for the entire data set and the five regions. n is the number of stations per region.  $R^2$  is the fraction of the spatial variance explained by the partitioning into the five regions.





|                  | Europe<br>(n=2370) |       | Northeastern<br>(n=288) |       | Atlantic<br>(n=875) |       | Central-<br>Eastern<br>(n=236) |       | Alpine<br>(n=622) |       | Mediterranean<br>(n=349) |       | R <sup>2</sup> |
|------------------|--------------------|-------|-------------------------|-------|---------------------|-------|--------------------------------|-------|-------------------|-------|--------------------------|-------|----------------|
|                  | m                  | cv    | m                       | cv    | m                   | cv    | m                              | cv    | m                 | cv    | m                        | cv    |                |
| MAF              | 0.171              | 1.114 | 0.126                   | 0.939 | 0.137               | 0.981 | 0.037                          | 1.095 | 0.264             | 0.816 | 0.222                    | 1.223 | 0.140          |
| MAF <sub>α</sub> | 0.211              | 0.961 | 0.176                   | 0.655 | 0.166               | 0.875 | 0.047                          | 0.942 | 0.304             | 0.728 | 0.304                    | 0.938 | 0.173          |
| CV               | 0.518              | 0.492 | 0.386                   | 0.347 | 0.494               | 0.435 | 0.695                          | 0.583 | 0.516             | 0.381 | 0.571                    | 0.529 | 0.090          |
| CS               | 1.278              | 0.773 | 0.821                   | 0.779 | 1.216               | 0.882 | 1.59                           | 0.727 | 1.466             | 0.565 | 1.263                    | 0.785 | 0.047          |



250 Figure 2: Mean specific flood (MAF ( $\text{m}^3 \text{s}^{-1} \text{km}^{-2}$ )) (a), Coefficient of variation (CV) (b), Mean specific flood normalised to a catchment area of  $100\text{km}^2$  (MAF<sub>α</sub> ( $\text{m}^3 \text{s}^{-1} \text{km}^{-2}$ )) (c), and Coefficient of skewness (CS) (d). Colours represent the estimate partitioned into eight classes of equal frequency.



### 3.2 Seasonality and flood moments

255 As an indicator of flood processes, the average direction of seasonality  $\bar{\theta}$  and the strength of seasonality  $k$  are plotted in Figure 3 for each catchment (see Figure 3 in Blöschl et al., 2017, for the spatial distribution). The closer the points are to the edge of the circle the stronger the seasonality. Additionally, the magnitudes of  $MAF_{\alpha}$ , CV and CS are indicated as colours as in Figure 3. The red circles in Figure 3 highlight geographic regions that are roughly homogeneous with respect to seasonality and the magnitude of the estimated flood moments, which were identified by examining seasonality maps (Blöschl et al., 2017).

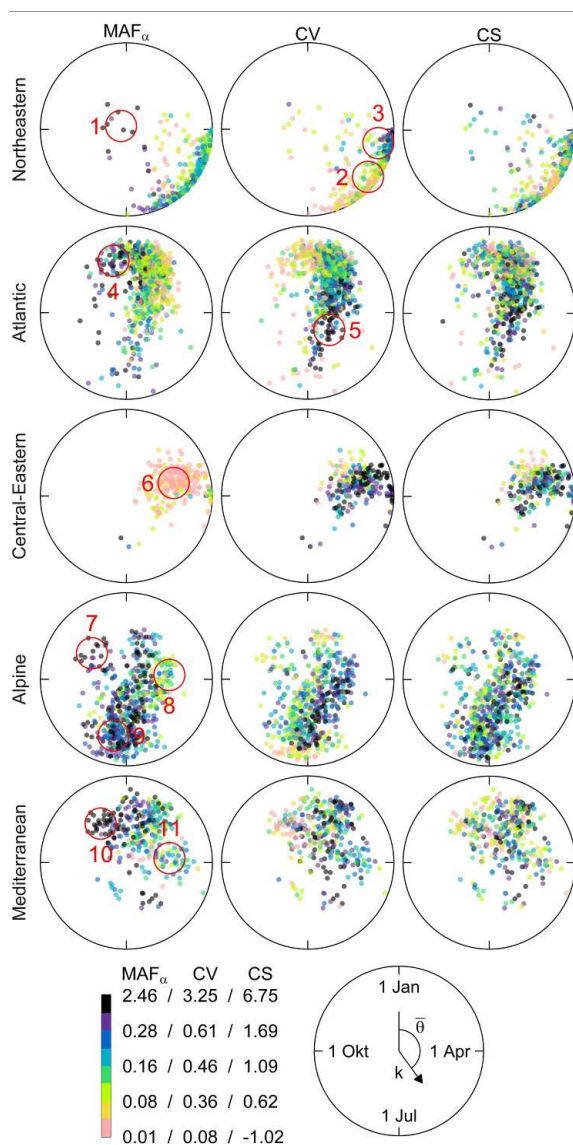
260 In Northeastern Europe floods mainly occur in spring and early summer with a strong seasonality reflecting the role of snowmelt.  $MAF_{\alpha}$  are in a medium range (green in Fig. 3) with the exception of the Norwegian coast (circle 1) where  $MAF_{\alpha}$  are much larger but with little seasonality because there is a mix of spring snow melt floods and winter rain floods (Kemter et al., 2020). The CVs of these catchments are small. On the other hand, floods in Western Russia almost always occur in April with large CV (circle 3). The June floods further in the  
265 North, adjacent to the White Sea, have much smaller CV because of a more consistent snow melt influence (Kemter et al., 2020, circle 2).

In the northwestern part of the Atlantic region (Ireland, west coast of the UK), floods tend to occur in December and the estimates of  $MAF_{\alpha}$  are large (circle 4). In the East of the Atlantic region (Southern Germany, Czech Republic, circle 5) the average occurrence of floods is in late spring, although the seasonality is weak but CVs  
270 are large.

In the Central-Eastern region (Poland, Ukraine, circle 6) where floods usually occur in spring, the  $MAF_{\alpha}$  are generally low and the CVs are large.

The catchments in the Alpine region with summer floods (circle 9) show high  $MAF_{\alpha}$  due to rainfall enhancement of the Alps. The catchments with autumn floods in Southern Austria and Slovenia (circle 7) exhibit very high  
275  $MAF_{\alpha}$  due to a stronger influence of the Mediterranean Sea. The region also contains the Carpathians and adjacent midlands (circle 8) where floods tend to occur in spring with lower MAF but rather high CV, likely because of a mix of snow, rain-on-snow and rainfall floods.

The Mediterranean region contains catchments with mostly winter floods with rather high  $MAF_{\alpha}$ . The autumn flood catchments in Slovenia have particularly high  $MAF_{\alpha}$  (circle 10) and low CV while the catchments with  
280 spring floods on the Balkans (circle 11) possess medium  $MAF_{\alpha}$  and CV.



285 Figure 3: Seasonality of annual flood peaks. Position in circle indicates mean date of occurrence (angle) and variability of the date (inverse of distance from centre). Each point represents one catchment. Colours of the points indicate flood moments as in Figure 2. Small red circles highlight subregions referred to in the text (1: Norwegian coast, 2: Northwestern Russia, 3: Western Russia, 4: Western UK and Southwestern Norway, 5: Southern Germany and North of Czech Republic, 6: Parts of Poland and Ukraine, 7: Southern Austria and Northern Slovenia, 8: Alpine and Carpathian midlands, 9: Alpine region, 10: Slovenia and Southern France, 11: Balkans)



290 **3.3 Scaling of flood moments with catchment area**

The first control on the flood moments examined here is catchment area as it is often the dominant and best understood control (Table 3, Fig. 4). The highest decrease in the mean annual flood (MAF) with catchment area occurs in the Mediterranean and the Alpine region with  $\beta_{MAF} = -0.255$  and  $-0.208$ , respectively, while the weakest the smallest decreases occur in the Northeastern and Central Eastern regions ( $\beta_{MAF} = -0.163$  and  $-0.108$ ) where snow melt is important. The coefficient of variation of the flood records (CV) decreases with catchment area in most regions. Again, the strongest decrease occurs in the Mediterranean while in the Northeastern and Central Eastern there is no significant relationship. There are few small catchment in the Central-Eastern region, which may make the regression with area less robust. Overall there is a tendency for CS to decrease with catchment area and the strongest decrease occurs again in the Mediterranean.

300

Table 3: Dependence of the flood moments with catchment area in a double logarithmic relationship Eq. (5) and analogous equations for CV; and a semi logarithmic relationship for CS, i.e.  $CS = \log A \beta_{CS}$ . Last lines show the 5% and 95% quantiles of catchment area (km<sup>2</sup>). \* indicates statistical significance (two-sided t-test) at the 5% level.

|   | Europe   | Northeastern | Atlantic | Central-Eastern | Alpine  | Mediterranean |
|---|----------|--------------|----------|-----------------|---------|---------------|
| $\beta_{MAF}$                                 | -0.245*  | -0.163*      | -0.184*  | -0.108*         | -0.208* | -0.255*       |
| $\beta_{CV}$                                  | -0.030*  | -0.015       | -0.042*  | 0.025           | -0.020* | -0.072*       |
| $\beta_{CS}$                                  | -0.133*  | -0.054       | -0.124*  | 0.280*          | -0.177* | -0.232*       |
| 5% / 95% quantiles of area (km <sup>2</sup> ) | 35/11500 | 28/18010     | 37/5331  | 142/32509       | 26/4212 | 47/27251      |

305

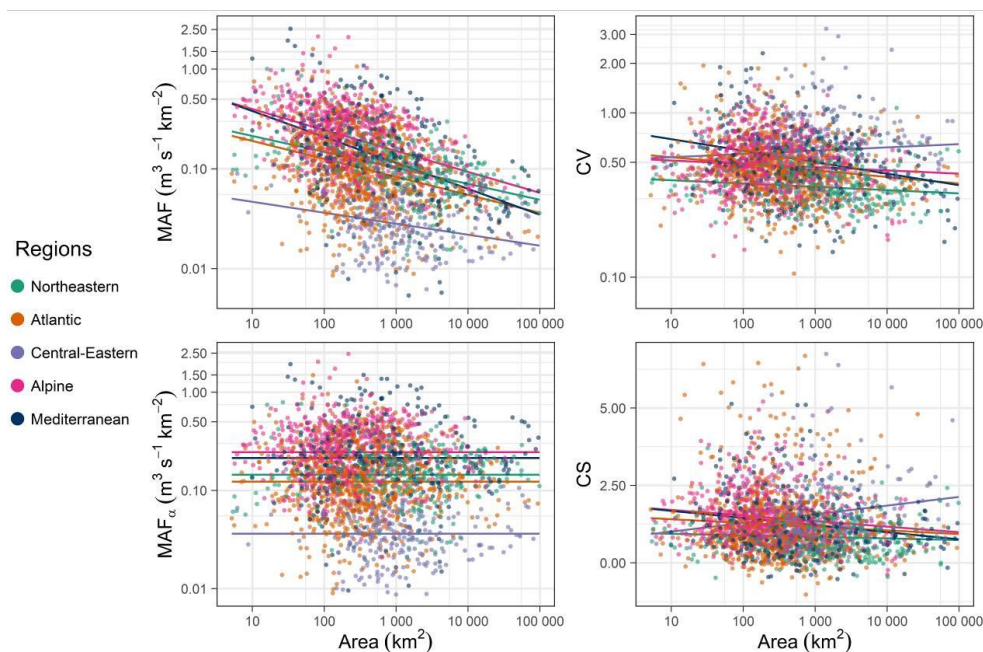


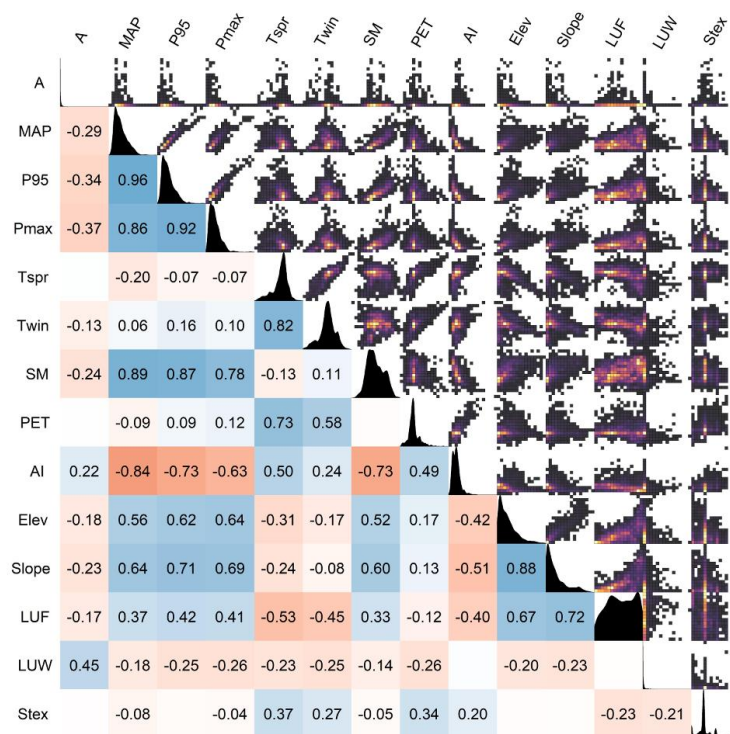
Figure 4: Mean annual specific flood (MAF), normalised mean annual specific flood (MAF<sub>a</sub>), coefficient of variation (CV) and coefficient of skewness (CS) plotted against catchment area (km<sup>2</sup>). Colours indicate region. Lines are regression lines for each of the regions.

310

### 3.4 Individual controls on flood moments

When interpreting the association of climate and catchment attributes with flood characteristics, it is important to account for the correlation between the attributes themselves which may mask causal relationships. Spearman correlation coefficients have therefore been estimated among all explanatory variables (Figure 5). The largest correlations occur among the precipitation characteristics, all of which are at least  $r=0.86$ . The correlation between long-term mean precipitation (MAP) and daily precipitation not-exceeded 95% of the time (P95) is even 0.96, indicating that the spatial patterns of these two variables in Europe are almost identical. The correlation between soil moisture (SM) and the precipitation variables is at least 0.78, and the correlation between the aridity index (AI) and the precipitation variables varies between -0.63 and 0.84. The latter may be partly related to the fact that AI is the ratio of potential evaporation (PET) and MAP. PET is related to spring temperature ( $r=0.73$ ). Elevation and slope are closely related to each other ( $r=0.88$ ) and they are also closely related to the precipitation variables with  $r$  of at least 0.56, reflecting orographic influences on precipitation. Forest cover (LUF) is related to elevation and slope ( $r=0.67$  and  $0.72$ , respectively) reflecting the presence of forest in mountain areas. The positive correlation between lake area fraction (LUW) and catchment area ( $r=0.45$ ) results from a tendency for large catchments to contain lowlands where lakes are more frequent than in the mountains, and the positive correlation between soil type (Stex) and spring temperature (Tspr) ( $r=0.37$ ) is due to coarse soils prevailing in the (colder) north of Europe. Fig. 5 also shows 2d histograms of the variables as well as their kernel density estimates.

325



330 Figure 5: Correlation between explanatory variables as in Table 1. For each variable the data consist of  $n=2370$  values, i.e. the number of catchments. Lower triangle: Spearman correlation coefficients. They are shown if they are statistically significant ( $\alpha=0.05$ ). Blue and red indicate positive and negative relationships, respectively. Upper triangle: 2d-histograms with colours indicating the frequency of observations in the bins (dark: few; bright: many, separate scale for each panel). Diagonal: kernel density estimate. All scales are linear.

335

Figure 6 gives the Spearman correlations of the flood moments  $MAF_\alpha$  and CV with catchment attributes. We mainly examine  $MAF_\alpha$  instead of  $MAF$  in order to minimise the effect of spatial differences in the catchment area on the correlations with the flood moments that may mask the direct effects of other variables. The correlations for CS are often weaker and more difficult to interpret, at least partly due to estimation uncertainty.

340 The corresponding correlations for  $MAF$  and CS with catchment attributes are given in Table A.1.5 in the Appendix.

While the correlations between  $MAF_\alpha$  and catchment area are of course small in all regions (Table 4), the correlations between  $MAF$  and catchment area (Table A.1.5, appendix) are significant in all regions ranging between 0.31 and 0.48, with the exception of central Eastern where it is only 0.23 which may be related to the more important role of snowmelt. Overall in Europe the relative large explanatory power of catchment area points to an important role of scale effects, although in most regions it is not the variable with the largest  $r$ .

345

$MAF_\alpha$  is significantly positively correlated with MAP in all regions (Figure 6) and the correlations with P95 and Pmax are similar. These high correlations may reflect the effect of rainfall, soil moisture as well as landscape evolution (Perdigão and Blöschl, 2014) as all rainfall variables as well as soil moisture are highly inter-correlated



350 (Figure 5). The correlations between  $MAF_{\alpha}$  and precipitation (both MAP and P95) are largest in the Atlantic  
region, reflecting the dominant role of precipitation in explaining the spatial variability of  $MAF_{\alpha}$  in this part of  
Europe. CV is significantly negatively correlated with MAP, P95 and Pmax, for almost all regions. The strongest  
relationship is observed in the Alpine and Mediterranean region. In drier catchments the occurrence of floods is  
more irregular (large CV, e.g. in Spain) as opposed to wetter catchments where every year rather large floods  
355 occur (small CV e.g. in Norway).

One would expect the strongest correlations between flood moments and temperature in the regions with  
important snow melt contributions (Northeastern, Central-Eastern regions) and this is actually the case (Figure  
6). Spring (March-May) and winter (December-February) temperature are negatively correlated with  $MAF_{\alpha}$  and  
positively correlated with CV.

360 The correlations between the flood moments and mean annual maximum monthly soil moisture (SM) are very  
similar to those with MAP as the two covariates are correlated with  $r=0.89$ . There are high positive correlations  
of  $MAF_{\alpha}$ , in particular in the Atlantic and the Mediterranean, and correspondingly strongly negative correlations  
between CV and soil moisture. On the other hand, there is a small negative correlation between  $MAF_{\alpha}$  and the  
mean annual potential evapotranspiration (PET) in all regions, which can be interpreted in PET generally  
365 reducing the antecedent wetness conditions of floods and hence the flood discharges. More striking are the CVs  
that are strongly positively correlated with PET in most regions with  $r$  ranging between 0.1 and 0.7. The aridity  
index (AI), defined as the ratio of PET and MAP has correlations ranging around those of PET and/or the inverse  
of MAP (i.e.  $-r$ ). The highest values of AI are observed in the Mediterranean region, where high correlations (in  
absolute value) are observed for all flood moments.

370 Mean catchment elevation (Elev) and mean topographic slope (Slope) are highly correlated with each other ( $r=$   
0.88) and therefore have similar correlations with the flood moments in most regions.  $MAF_{\alpha}$  is highly positively  
correlated with both elevation and slope across all regions of Europe similar to the rainfall variables, pointing to  
an indirect effect of topography on mean floods through precipitation. This is consistent with high correlations of  
elevation and slope to the precipitation variables (around 0.6 and 0.7, respectively, Fig. 5).

375  $MAF_{\alpha}$  is positively correlated with the fraction of area covered by forest (LUF) in all regions and negatively  
correlated with the fraction of area covered by water bodies, i.e. lakes and reservoirs, (LUW) in most regions,  
including in the region with the largest fraction of water bodies (the Northeastern region where the median LUW  
is 5.7%). The positive correlation between  $MAF_{\alpha}$  and LUF is most likely due to an indirect relationship, as areas  
with high forest cover tend to be high-elevation regions such as mountains, where precipitation is augmented  
380 through orographic effects.

While there is little correlation between  $MAF_{\alpha}$  and soil texture, there is a clear effect of soil texture on CV with  
finer soils (Stex=5) being associated with higher CVs than coarse soils (Stex=1).



|       | Europe           |       | Northeastern     |       | Atlantic         |       | Central – Eastern |       | Alpine           |       | Mediterranean    |       |
|-------|------------------|-------|------------------|-------|------------------|-------|-------------------|-------|------------------|-------|------------------|-------|
|       | MAF <sub>α</sub> | CV    | MAF <sub>α</sub> | CV    | MAF <sub>α</sub> | CV    | MAF <sub>α</sub>  | CV    | MAF <sub>α</sub> | CV    | MAF <sub>α</sub> | CV    |
| A     | -0.12            | -0.13 |                  | -0.16 |                  | -0.19 |                   |       |                  |       |                  | -0.25 |
| MAP   | 0.59             | -0.33 | 0.15             | -0.23 | 0.67             | -0.33 | 0.24              | -0.49 | 0.26             | -0.61 | 0.48             | -0.68 |
| P95   | 0.60             | -0.22 |                  |       | 0.66             | -0.22 | 0.31              | -0.19 | 0.24             | -0.58 | 0.52             | -0.59 |
| Pmax  | 0.55             | -0.05 |                  |       | 0.52             | 0.14  | 0.22              | -0.18 | 0.26             | -0.40 | 0.49             | -0.36 |
| TSpr  | -0.22            | 0.26  | -0.35            | 0.58  | -0.29            |       |                   | 0.50  | -0.14            | 0.38  | -0.12            | 0.17  |
| TWin  | -0.07            | 0.04  | -0.20            | 0.20  |                  | -0.23 | -0.33             | -0.52 | -0.10            | 0.10  |                  | 0.27  |
| SM    | 0.57             | -0.31 | 0.16             | -0.14 | 0.55             | -0.29 | 0.28              | -0.40 | 0.22             | -0.56 | 0.50             | -0.64 |
| PET   |                  | 0.39  | -0.33            | 0.60  | -0.22            | 0.34  |                   | 0.68  | -0.11            | 0.11  | -0.21            | 0.63  |
| AI    | -0.53            | 0.46  | -0.36            | 0.62  | -0.53            | 0.38  |                   | 0.63  | -0.31            | 0.50  | -0.43            | 0.69  |
| Elev  | 0.55             | 0.08  | 0.47             | -0.31 | 0.44             | 0.35  | 0.50              | 0.21  | 0.16             | -0.47 |                  | 0.20  |
| Slope | 0.65             |       | 0.39             | -0.36 | 0.62             | 0.17  | 0.30              |       | 0.24             | -0.40 | 0.37             |       |
| LUF   | 0.45             | -0.10 | 0.28             |       | 0.45             | 0.14  |                   | -0.39 | 0.16             | -0.26 | 0.32             |       |
| LUW   | -0.16            | -0.27 | -0.21            | -0.22 |                  | -0.20 | -0.55             | -0.50 |                  | -0.19 |                  | -0.19 |
| Stex  | -0.06            | 0.29  |                  | 0.37  |                  | 0.17  | 0.32              | 0.53  |                  | 0.23  | -0.18            | 0.26  |

385 Figure 6: Spearman-Correlation between statistical moments of flood series (mean specific discharge normalized to a  
 catchment area MAF<sub>α</sub> of α=100km<sup>2</sup> and the coefficient of variation CV) and catchment attributes. Correlations are shown if  
 they are statistically significant (α=0.05). Blue and red indicate positive and negative relationships, respectively. The  
 correlations for mean specific discharge MAF and coefficient of skewness CS with catchment attributes are given in Table  
 A.1.5.

390





### 3.5 Multiple controls on the flood moments

While Figure 6 examines the relationships between flood moments and single covariates using Spearman correlation coefficients, in this section we test the relationship between flood moments and multiple covariates with regression models applied for each of the regions separately. Thus the covariates with the largest contributions are those that explain most of the  $R^2$  of the spatial variability of the flood moments within each of the regions. We used MAF, rather than  $MAF_a$ , in order to avoid prior assumptions regarding the role of catchment area. Given that CS was correlated with fewer covariates than the other flood moments we focused here on MAF and CV (Table A.1.5). We represent each of four most important groups of covariates (area, precipitation, temperatures and water balance) by one covariate. The contributions to explaining the spatial variability of MAF in terms of the normalised general dominance measure (nGDM) are shown in Figure 7 and Table A.1.3 and are discussed below by region.

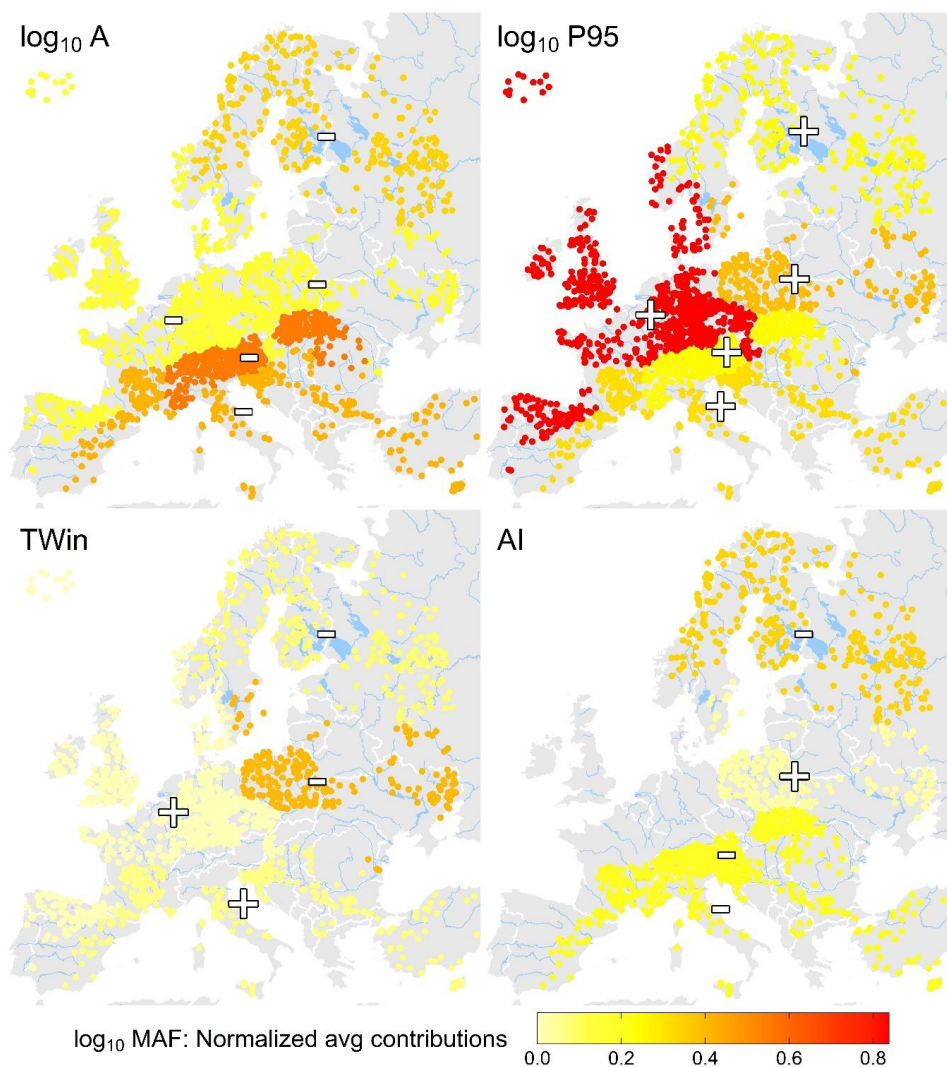
In Northeastern Europe, like in all regions, catchment area is an important predictor of MAF. Additionally, P95 and AI play an important role representing an East-West gradient with the largest MAF, largest P95 and the lowest AI in Norway.

In the Atlantic region, P95 is by far the most relevant covariate (nGDM= 0.8) as one would expect in a region where floods are rainfall driven and soil moisture tends to be high in the flood season (winter) (Blöschl, Hall et al., 2019 ; Kemter et al., 2020).

In the Central-Eastern region MAF is generally low with little spatial variability. The corresponding  $R^2$  is small (Table A.1.1), as it is harder to explain the small spatial contrast. The largest contribution is winter temperature and P95. Negative coefficients for winter temperature point to lower temperatures driving deeper snow packs and higher floods.

In the Alpine region area is most important and in fact relatively more important than in any other region. However, the  $R^2$  of the model in the Alpine region is low.

In the Mediterranean catchment area is important (nGDM= 0.43), which is due to the small coastal catchments exhibiting much larger specific floods than the larger catchments that extend further into the land, e.g. in Catalonia, Liguria, Slovenia (e.g. Gaume et al., 2009). Additionally, P95 plays a relevant role.



420 Figure 7: Results of dominance analysis for regional regression models for MAF. Panels depict the average contributions  
(normalised general dominance measure, nGDM) of the covariates included in the regressions (log of catchment area, log of  
extreme precipitation index P95, mean winter temperature and aridity index). Plus- and Minus-signs indicate sign of the  
regression coefficients.

425 For CV (Figure 8, Table A.1.4), in the Northeastern region the Aridity index (AI) is the most important covariate  
by far. This is due to Scandinavia being much wetter than Northwestern Russia translating into lower CVs.

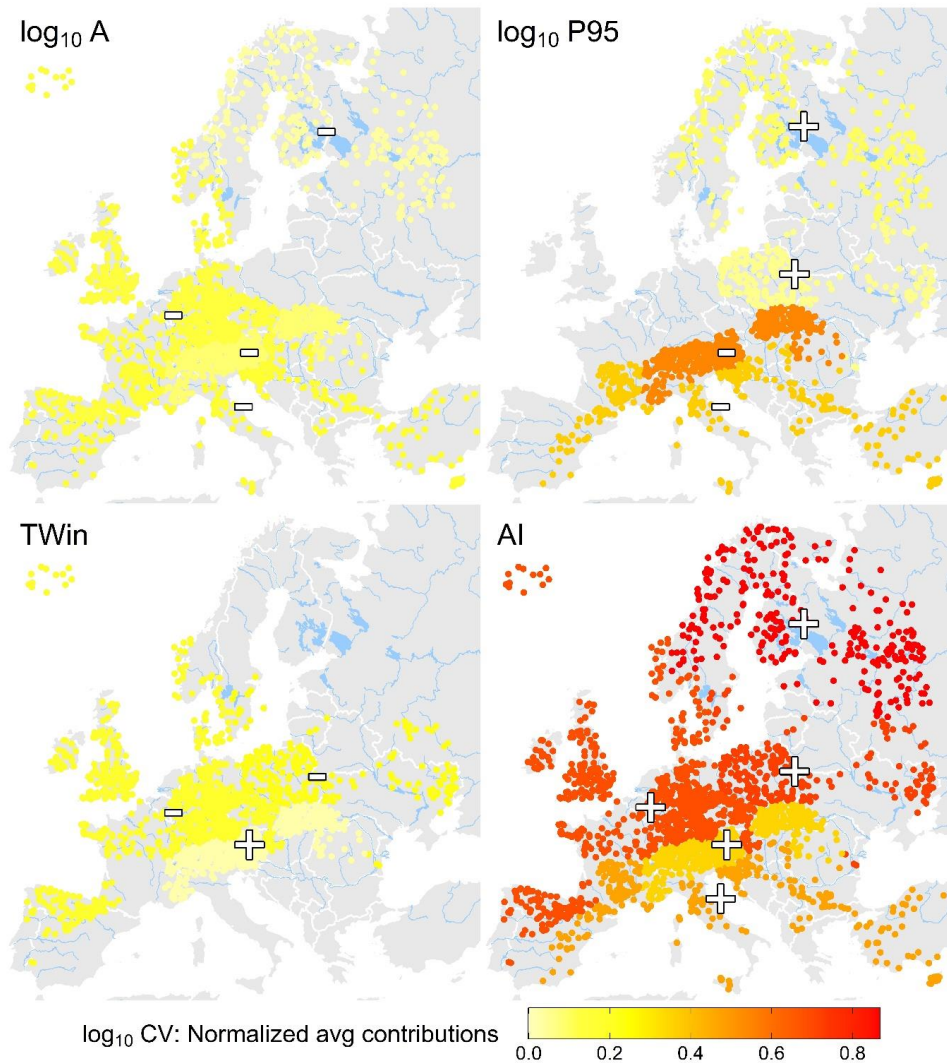
In the Atlantic region AI is the most important variable for explaining the spatial variability of CV although the  
overall explanatory power of the regional model is rather low ( $R^2$  of 0.27, Table A.1.2). The smaller CV closer to  
the ocean in the Atlantic region is partly explained by higher winter temperatures.



In the Central-Eastern region AI dominates again with higher CV in the Ukraine correlated with higher aridity  
430 than further in the West, both due to higher PET and lower MAP.

The Alpine region is an exception in that P95 explains more spatial variability of CV than AI (nGDM of 0.54  
and 0.35, respectively). This is because PET is negatively related to elevation but the flood magnitudes are  
controlled by the higher orographic rainfall on the windward (NW) side of the Alps.

In the Mediterranean both aridity and P95 are important predictors. For example, low aridity (because of high  
435 MAP) in Croatia and Slovenia is associated with low CV, and high P95 in Southern France is associated with  
moderately low CV.



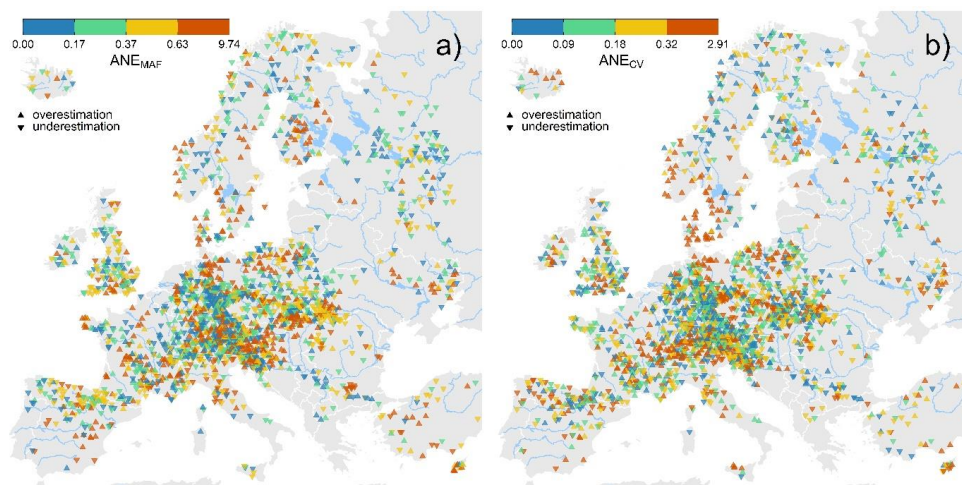


440 Figure 8: Results of dominance analysis for regional regression models for CV. Panels depict the average contributions (normalised general dominance measure, nGDM) of the covariates included in the regressions (log of catchment area, log of extreme precipitation index P95, mean winter temperature and aridity index). Plus- and Minus-signs indicate sign of the regression coefficients.

### 3.6 Estimating flood moments from multiple controls

In this section we analyse how well the regression models of the previous section (where A, P95, TWin and AI were used as covariates) are able to predict the moments at any location in terms of leave-one-out-cross-validation (Figures 9 and 10). Overall there is a tendency of MAF to be overestimated in those areas where the observed values of MAF are small (e.g. Hungary and Denmark), and underestimated where they are large (e.g. Carpathians, Northern Italy) reflecting the property of spatial estimators to underestimate spatial extremes. The overestimation in Finland may also be due to lake retention not being captured in the model. To some degree CV is also overestimated in areas of low CV (e.g. southern Norway and Denmark) and underestimated in areas of high CV (e.g. Ukraine, Ore mountains) although there are also large CV areas it is overestimated (e.g. Southern Spain). The errors are smallest in Russia, Central Germany, British Island and France where the spatial gradients in CV are relatively smooth.

450 The median absolute normalized error of MAF and CV is 0.37 and 0.18, respectively, with 25%-quantiles of 0.17 and 0.09 and 75%-quantiles of 0.63 and 0.32. This means that the absolute normalized error of CV is about half that of MAF, which seems to be related to the relatively smaller spatial variability of CV as compared to MAF (spatial cvs of 1.11 and 0.49, respectively, Table 2).



460 Figure 9: Absolute normalised errors  $ANEMAF$  and  $ANECV$  of the predictions of the regional regression models for MAF and CV. Errors are evaluated on scale of data (not logarithmised). Colours refer to binned classes of equal frequency. Triangles facing upwards indicate gauges where the model overestimates the moments, triangles facing downwards where the model underestimates.

465 Figure 10 depicts the predicted (leave-one-out) MAF and CV using the regressions (Circles in Figure 10, Tables A.1.1 and A.1.2) and the predicted MAF and CV by spatial proximity through kriging of the observed moments (background colour). Predictions are shown on the scale of the data (not logarithmised) using the colour scale



from figure 2. Notwithstanding the relatively large ANE (Fig. 9), the overall patterns of the moments are very similar to the observed ones (Figure 2). Notice that the regression models are not applied for all available sites because some of the local peculiarities (that may have physical reasons) are missed. Overall, the patterns of the moments are consistent with the process reasoning put forward in this paper.

470

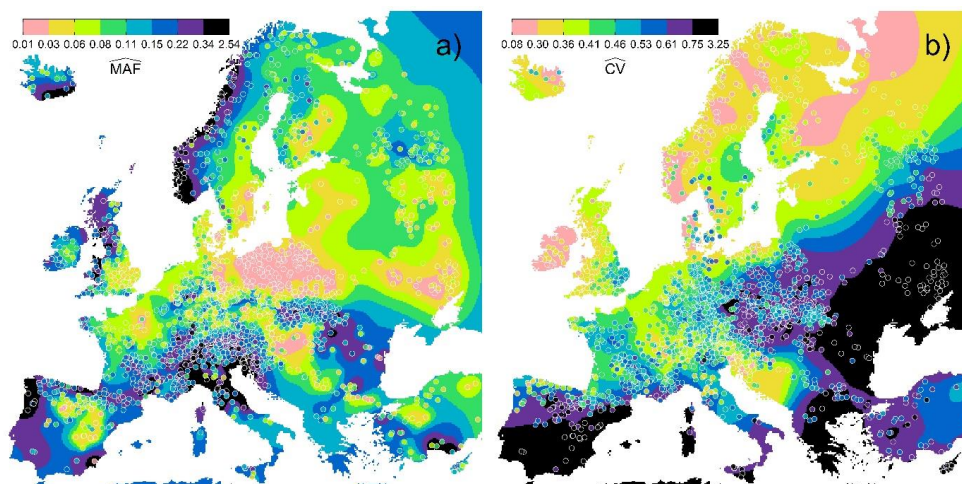


Figure 10: Predicted values of regional regression models and ordinary kriging for MAF ( $\text{m}^3 \text{s}^{-1} \text{km}^2$ ) and CV. Circles refer to predictions of regression models, background refers to predictions of kriging. Colours refer to binned classes of equal frequency for original data (estimated statistical moments) as in Figure 2.

475

#### 4. Discussion and Conclusions

##### 4.1 Patterns of flood moments in Europe

Overall there are clear patterns of the flood moments across Europe. As would be expected MAF shows the clearest patterns while they are less clear for CV and particularly CS, at least partly because of sampling variability.

480

In the Atlantic region where floods mainly occur in winter as a result of moisture influx from the ocean,  $\text{MAF}_\alpha$  is very high (above  $0.5 \text{ m}^3/\text{s}/\text{km}^2$  at the West coasts of Norway, Scotland and Galicia, Fig. 2). The CVs, on the other hand, are small (typically around 0.3 at the Norwegian coast and in Scotland and 0.5 in Galicia) as the atmospheric moisture influx tends to be consistent between years (Giorgi et al., 2004). As one moves towards the continent from the west coast of the British Isles MAF tends to decrease and CV increase because of the decreasing moisture availability and floods tend to occur later in the year (i.e. Jan instead of Dec., Fig. 3).

485

Further inland, the various mountain ranges (Pyrenees, Massif Central, Alps Apennines, Ore mountains, Carpathians, Balkan mountains) stand out with higher MAF than the surroundings (mostly above  $0.3 \text{ m}^3/\text{s}/\text{km}^2$ ) and summer as the dominant flood season due to their effects of enhancing rainfall and probably shallower soils.

490

On the other hand, there are clear differences between the CVs of these mountain ranges. While CVs in the Alps and the southern Slovenian mountains are low, they are high in the Ore mountains and some of the other



mountain ranges which reflects the stronger influence of Mediterranean storm tracks (Hofstätter et al., 2018, Hofstätter and Blöschl, 2019) perhaps along with non-linear runoff generation (Viglione et al., 2009).

495 As one moves inland in the North of Europe from the Norwegian coasts towards the North European plain, MAF decreases to values around  $MAF_a=0.1 \text{ m}^3/\text{s}/\text{km}^2$  due to a decrease in the Atlantic influence and increase of snow processes resulting in late spring events with pronounced seasonality. As one moves southward from the Northeast, CV increases and flood seasonality decreases in line with the increased influence of rain-on-snow and rain floods which tend to be more irregular than snowmelt floods alone.

500 Some of the continental regions of Europe (Hungary, Poland, Ukraine) are particularly sheltered by mountain chains, resulting in low precipitation, both at the annual scale and for extreme events which translates into low MAF and mostly high CV.

In the Mediterranean, where floods tend to occur in autumn and winter, MAF is generally high, particularly in Southern France, Slovenia and Croatia, Liguria, and parts of northern Italy, as a result of the potential of heavy autumn storms due to the warm Sea. In most regions this also results in high CV, this is not the case in Slovenia and Croatia, due to the consistency of these storms between years (Xoplaki et al., 2004, Salinas et al., 2014b).

#### 4.2 Interpretation of controls of flood moments

510 The degree to which the moments change with catchment area is a fingerprint of the spatial variability of the flood producing processes (Merz et al., 2003, Sivapalan et al., 2005, Merz and Blöschl, 2009, Viglione et al., 2010ab) (Table 3, Figure 4). As expected, there is a strong scaling effect of MAF with area. The strongest decrease of MAF with area is observed for the Mediterranean region, which points to the important role of small scale, convective storms, patchy runoff generation processes, and more generally flash floods (Gaume et al., 2009; Marchi et al., 2010; Amponsah et al., 2018). On the other hand, the smallest decrease is found in the Central-Eastern and Northeastern region, where snowmelt is a dominant flood driver. Snowmelt tends to occur over larger regions simultaneously which results in a smaller reduction of MAF with catchment scale. This is consistent with Blöschl and Sivapalan et al. (1997) and Merz and Blöschl (2003). The relatively weak decrease in the Atlantic regions suggests an important role of large scale precipitation as would be expected (Kemter et al., 2020).

520 CV decreases with area in most of the regions. Again, the strongest decrease is observed for the Mediterranean region, which can be interpreted in terms of similar aggregation processes as in the case of MAF. Additionally, the degree of non-linearity in runoff generation may decrease with catchment size (Sivapalan, 2003) as threshold processes associated with Hortonian runoff generation or soil storage homogeneity may be more relevant in small catchments (Penna et al., 2011; Rogger et al. 2012). On the other hand, the smallest decrease occurs in the Northeastern region and in the Central Eastern region the estimated regression coefficient is even positive. While both relationships are not significant, they do point towards the larger scale of snowmelt processes relative to other flood generation processes along with more linear runoff generation processes and the larger role of baseflow (Blöschl and Sivaplan, 1997).

The strongest Spearman correlation for MAF (in absolute value) is observed for the Mediterranean region, while the weakest is observed in the Central-Eastern region (Table A.1.5), in line with the difference in the scale



530 dependence between these two regions (Table 3). For CV (Figure 6) the spatial differences of the correlations  
between the regions are also consistent with the scaling regressions of Table 3 but, overall, they are smaller than  
those of MAF. This may be related to possible non-monotonous relationships between CV and area as suggested  
by Smith (1992), and more complex aggregation effects (Blöschl and Sivapalan 1997). The weakest relationship  
is found in Central Eastern Europe where snow is important, and in the Alpine region where the spatial  
variability of other controls is particularly large ( $r=0.09$  and  $-0.03$ , respectively).

535 As compared to the other controls on the flood moments, area plays an important role for MAF but less so for  
CV (Table A.1.5, Figures 7 and 8). In the Alpine region the Spearman correlations between MAF and area are  
larger than those between area and other covariates (Table A.1.5) and it has the large contributions to the fit of  
the regional model (Figure 7). However, this may not be because of the high explanatory power of area but of  
540 the lower explanatory power of the other covariates likely related to the complex topography. For CV, area has  
some explanatory power in the Atlantic and Mediterranean regions (Figure 6) and is used in most regional  
regression models, but the role of climate variables such as precipitation and aridity is always much higher than  
that of area (Figure 6, Figure 8) suggesting that aggregation effects are relatively less important at the European  
scale than at the regional scale.

Precipitation characteristics are represented by three variables in the present study, which are strongly correlated  
545 among themselves (Figure 5). The Spearman correlations between MAF and the precipitation characteristics are  
positive for Europe and in individual regions while for CV and precipitation they are negative (Figure 6) but  
there are some differences between the precipitation variables. MAP is a surrogate for event precipitation,  
antecedent soil moisture and landscape evolution, whereas P95 and Pmax are more representative of  
characteristics of event precipitation. Pmax is representative of a more extreme part of the daily precipitation  
550 distribution than P95 (typically Pmax is twice the value of P95, Table 1). The correlations of MAP and P95 with  
MAF<sub>a</sub> are similar, but generally larger than that of Pmax which may be due to Pmax capturing antecedent soil  
moisture less. Mimikou and Gordios (1989) and Merz and Blöschl (2009) concluded that MAP was somewhat  
superior to other precipitation variables in explaining the spatial MAF variability in Greece and Austria, but at  
the European scale the predictive power of MAP and P95 are similar, and that of Pmax is slightly lower.

555 CV is always a better correlated with MAP than with P95 and Pmax reflecting the decreasing degree with which  
antecedent soil moisture is captured as one moves from MAP to P95 and Pmax. Drier catchments have the  
ability to produce larger CVs because some of the events may be a combination of both large precipitation and  
wet initial conditions such producing much larger floods than usual (Farquharson et al., 1992, Viglione et al.,  
2009; Kemter et al., 2020). This effect is also represented in the negative correlations between CS and MAP ( $r=-$   
560  $0.35$ ) and CS and P95 ( $r=-0.34$ ) (Table A.1.5) in the Mediterranean which is related to a particularly large  
potential for this contrast in initial conditions.

In the context of multiple controls, rainfall (in this case only P95 was considered) is always among the important  
variables for explaining MAF (Figure 7). However, in the case of CV, aridity is vastly more important, as the  
combination of evaporation and precipitation better captures the typical initial condition state of the catchments  
565 before floods.



Mean spring and winter temperature were used in the analysis to capture snow processes. As would be expected, the Spearman correlations between temperature and  $MAF_{\alpha}$  and CV are comparatively high in the Northeastern and Central-Eastern region, where snow-processes are important for floods. Temperatures are negatively correlated with  $MAF_{\alpha}$  and positively correlated with CV. The colder it is, the more precipitation is stored as snowpack in winter, leading to, on average bigger snowmelt floods in spring/early summer, but they are less variable (smaller CV) which may be related to the smaller interannual variability of air temperature as compared to that of precipitation (Giorgi et al. 2004). Snowmelt floods are physically limited by the amount of water stored as snow and solar radiation. This upper limit is also contributes to less extreme and more regular floods (Merz and Blöschl, 2003). In these cold regions temperatures are better correlated with  $MAF_{\alpha}$  and CV than with the precipitation variables and almost as well as with aridity, although this depends on the moment and the region.

Winter temperatures add explanatory power to the regional regression models of  $MAF$  in the Central-Eastern region, but a rather small contribution for the other regions (Figure 7). For CV, temperatures explain some of the spatial variability in the Central-Eastern and the Atlantic region, but generally its contribution is low (Figure 8). On the one hand, winter temperature may not be a perfect proxy for the spatial distribution of flood-relevant snowmelt. On the other hand, the other variables may more directly capture runoff generation processes.

Soil moisture, PET and the aridity index (AI) are related to long-term water balance characteristics and are significantly correlated with the estimated flood moments for almost all regions. Soil moisture is positively correlated with  $MAF_{\alpha}$  and negatively correlated with CV, whereas the opposite holds for PET and AI. Soil moisture and MAP are highly correlated, which is related to soil moisture being driven by long term precipitation. The lower the wetness state, the more room for variations in the runoff coefficients between years, and therefore flood peaks and thus high CV (Viglione et al., 2009). For PET and AI the highest correlations with  $MAF_{\alpha}$  are observed in the Northeastern, the Atlantic and the Mediterranean region. AI is strongly correlated with CV (Figure 6) and a particularly important variable for capturing the spatial variability of CV in regional regression models (Figure 8). High aridity implies a combination of low precipitation and high evaporation, leading to comparatively dry antecedent conditions. AI may also capture the non-linearity of runoff-generating mechanisms relevant for CV (Blöschl and Sivapalan, 1997). Additionally, precipitation tends to be more variable in the arid regions of Europe (e.g. Giorgi et al., 2004), so there may be both a precipitation and runoff generation effect, the latter being related to the stronger randomness of the runoff coefficient. The effect of the large variability of runoff coefficients between years in the arid catchments of Europe (large AI) is also apparent in the positive correlations with CS in the Mediterranean and Central-Eastern region ( $r=0.35$  and  $0.50$ , respectively) (Table A.1.5)

Topography is included via slope and elevation in the present analysis, but the observed effects of topography on the flood moments are most likely indirect. Precipitation characteristics are highly correlated with topographical indices (Figure 5) and their spatial patterns are very similar (not shown), suggesting little unique effect. Faster routing (flow velocity) due to topography does not seem to be a relevant factor for the spatial patterns of flood moments at the European scale, given that response times may be more closely related to geology than topography at the regional scale (Gaál et al., 2012).





The fraction of area covered by forest (LUF) is positively correlated with  $MAF_a$  which is not consistent with the usual expectation of higher infiltration capacities and therefore smaller floods peaks for forest soils (Sun et al., 605 2018). At the European scale, apparently, this effect is masked by the correlations between forest cover and precipitation. In high elevation regions of Europe forest cover tends to be high as these areas have not been deforested for agricultural purposes, and these are also the areas of high rainfall because of topographic effects on rainfall. Additionally, runoff coefficients may be higher in these high rainfall areas due to shallower soils and water tables notwithstanding the forest cover (Merz et al., 2006, Rogger et al., 2017).

610 The fraction of area covered by water bodies reduces both  $MAF_a$  and CV. The former is consistent with retention effects while the relationship between CV and water body size may be non-linear (increasing CV up to a water body threshold and decreasing CV beyond, Wang et al., 2017) which is not captured by Spearman correlation.

Soil texture, when interpreted in terms of pedotransfer functions (Picciafuoco et al., 2019), is expected to affect 615 infiltration of event rainfall. Coarse soils ( $Stex=1$ ) are therefore expected to be associated with smaller  $MAF_a$  than fine soils ( $Stex=5$ ) but the data show no consistent relationship. In a similar vein, the data suggest that coarse soils tend to be associated with small CV, which contrasts what one would expect by reasoning in terms of runoff generation processes. For coarse soils one would expect that, for small events, most of the water infiltrates but when a threshold is exceeded the rainfall starts to run off from the surface, thus leading to larger 620 CV relative to soils without threshold behaviour (Rogger et al., 2013). One reason for observing the opposite are the correlations between MAP and  $Stex$  within the regions which range between -0.08 and -0.36, i.e., coarse soils would be associated with high precipitation which would explain large MAF and small CV. Apparently at the scale of an entire continent, the soil characteristics (at least the texture available here) are less important than climate variables. The rather low explanatory power of soil texture and land use for hydrological response at 625 the regional scale is a general concern that also affects the estimation of other variables in the context of predictions in ungauged basins (Blöschl et al., 2003).

#### 4.3 Implications

Even though the main objective of this paper is to investigate why spatial patterns of flood moments occur, the results in Section 3.6 may be considered as a benchmark for flood moment estimation in ungauged basins at the 630 European scale. The median absolute normalized error (ANE) of MAF and CV is 0.37 and 0.18, respectively. This is relatively large as compared to similar, but smaller scale, studies in the literature (Merz and Blöschl, 2009; Viglione et al., 2013). The fit of the regional models changes between the regions, which reflects the relative importance of the flood generating processes changes between the regions. For the case of MAF,  $R^2$  is largest in the Atlantic and Mediterranean regions (Table A.1.1) and for CV it is largest in Eastern and 635 Mediterranean regions. Clearly there is no one-fits-all model. The regions here were derived based on previous climatic partitions of Europe and the goal of homogeneity with respect to flood generating processes and geographic coherence, rather than optimal predictive performance of the regional models.

Overall, the findings of this paper suggest that, at the continental scale, climate variables dominate over land surface characteristics as control of the spatial patterns of flood moments. Given the evidence for the 640 coevolution of landscape and climate (Perdigao and Blöschl, 2014, Troch et al., 2015) but the general lack of



645 predictive power of variables related to land use, soil and geology for hydrological quantities (Merz and Blöschl, 2009, Rogger et al., 2017), there is a need for new types of land characteristics, that are consistent across countries. Merz and Blöschl (2009) illustrate this notion by a comparison of two Austrian catchments that have strikingly similar geological characteristics in terms of percentage of area of certain geological types, but vastly different rainfall-runoff response-behaviour. At the plot, hillslope and catchment scales, runoff generation is strongly controlled by soil properties, which control infiltration and saturation capacities (Peschke and Sambale, 1999; Scherrer et al., 2007; Rogger et al., 2012; Picciafuoco et al., 2019). There have been attempts to relate or upscale local soil characteristics and regional ones (e.g., Schmocker-Fackel et al., 2007). One successful example is the HOST classification used in the UK (Boorman et al., 1995; Lilly et al., 1998; Maréchal and Holman, 2005), which has been demonstrated to be able to capture runoff generation processes and their spatial variability. Of course, scaling becomes important as well and land-use may have larger explanatory power in small catchments than in larger ones (Viglione et al., 2016).

655 The finding that climate is the main control for the spatial variability of the flood moments, within the range of the variables considered, also has some implications for quantifying the temporal flood variability. If the spatial patterns of flood behaviour at the continental scale are primarily driven by climatic influences, their temporal fluctuations might be propagated to floods (Šraj et al., 2016, Blöschl, Hall et al., 2019, Bertola et al., 2020, Kemter et al., 2020) On the other hand: flood changes of small local streams may be much more controlled by land use change such as urban development and deforestation (Rogger et al., 2017). One should however be careful in trading space for time in the context of change, i.e. in assuming that future flood characteristics in one region will be similar to the present ones in another region because the climate in the former will be similar to the present climate in the latter. This is because of the space-time asymmetry discussed in Perdigao and Blöschl (2014), i.e. the fact that, because of the celerity of coevolution, spatial and temporal statistics are not necessarily the same.

665 Hydrology of flood frequency is challenging because it deals with the extreme limit of the natural variability of river flows. This paper is a step toward a better understanding of the hydrology of flood frequency, along with studies that combine process hydrology, comparative hydrology and paleohydrology, including learning the recent past history of floods (Merz and Blöschl, 2008ab, Viglione et al., 2013, Blöschl et al., 2020). We believe that linking the hydrology of flood frequency to models of coevolutionary indices of climate and landscape has the potential to reveal a lot about all aspects of catchment hydrology, ultimately leading to better predictions.

670

675



## 5. Appendix

Table A.1 Regression coefficients (standard errors), model error variance and  $R^2$  of regional regression models for MAF

| Log <sub>10</sub> MAF | (Intercept) | Log <sub>10</sub> A | Log <sub>10</sub> P95 | TWin        | AI          | sigma | R <sup>2</sup> |
|-----------------------|-------------|---------------------|-----------------------|-------------|-------------|-------|----------------|
| Europe                | -2.18(0.09) | -0.16(0.01)         | 1.61(0.07)            | -0.02(0.00) | -0.04(0.02) | 0.31  | 0.47           |
| Northeastern          | -1.76(0.42) | -0.14(0.02)         | 1.22(0.31)            | -0.05(0.01) | -0.33(0.08) | 0.24  | 0.41           |
| Atlantic              | -3.31(0.11) | -0.13(0.01)         | 2.54(0.09)            | 0.01(0.00)  |             | 0.26  | 0.51           |
| Central-Eastern       | -4.54(0.62) | -0.09(0.03)         | 3.33(0.59)            | -0.07(0.01) | 0.10(0.07)  | 0.25  | 0.33           |
| Alpine                | -0.68(0.21) | -0.18(0.02)         | 0.47(0.14)            |             | -0.16(0.06) | 0.27  | 0.27           |
| Mediterranean         | -1.09(0.26) | -0.22(0.02)         | 0.94(0.19)            | 0.02(0.01)  | -0.16(0.04) | 0.32  | 0.47           |

680

Table A.2. Regression coefficients (standard errors), model error variance and  $R^2$  of regional regression models for CV

| Log <sub>10</sub> CV | (Intercept) | Log <sub>10</sub> A | Log <sub>10</sub> P95 | TWin        | AI         | sigma | R <sup>2</sup> |
|----------------------|-------------|---------------------|-----------------------|-------------|------------|-------|----------------|
| Europe               | -0.49(0.05) | -0.05(0.00)         | 0.06(0.03)            | 0.00(0.00)  | 0.22(0.01) | 0.15  | 0.29           |
| Northeastern         | -1.31(0.10) | -0.02(0.01)         | 0.54(0.08)            |             | 0.47(0.03) | 0.1   | 0.48           |
| Atlantic             | -0.40(0.02) | -0.05(0.01)         |                       | -0.02(0.00) | 0.21(0.01) | 0.14  | 0.28           |
| Central-Eastern      | -2.43(0.29) |                     | 1.42(0.29)            | -0.04(0.00) | 0.60(0.04) | 0.13  | 0.61           |
| Alpine               | 0.50(0.10)  | -0.05(0.01)         | -0.64(0.07)           | 0.01(0.00)  | 0.08(0.03) | 0.13  | 0.37           |
| Mediterranean        | 0.23(0.11)  | -0.08(0.01)         | -0.45(0.08)           |             | 0.12(0.02) | 0.14  | 0.55           |

Table A.3. Measure for general dominance (additional contributions) for MAF – indicating general dominance. For each row: highest value indicates most important variable in terms of improvement of the model fit for the given regression, second highest indicates second most important, lowest indicates least important. Summing over measures gives  $R^2$  of regression.

685

| Log <sub>10</sub> MAF | Log <sub>10</sub> A | Log <sub>10</sub> P95 | TWin | AI   | R <sup>2</sup> |
|-----------------------|---------------------|-----------------------|------|------|----------------|
| Europe                | 0.12                | 0.25                  | 0.01 | 0.09 | 0.47           |
| Northeastern          | 0.14                | 0.1                   | 0.03 | 0.14 | 0.41           |
| Atlantic              | 0.08                | 0.43                  | 0    |      | 0.51           |
| Central-Eastern       | 0.06                | 0.13                  | 0.13 | 0.01 | 0.33           |
| Alpine                | 0.15                | 0.07                  |      | 0.06 | 0.27           |
| Mediterranean         | 0.2                 | 0.15                  | 0.03 | 0.1  | 0.47           |



690

Table A.4. Measure for general dominance (additional contributions) for CV – indicating general dominance. For each row: highest value indicates most important variable in terms of improvement of the model fit for the given regression, second highest indicates second most important, lowest indicates least important. Summing over measures gives  $R^2$  of regression.

|                 | $\text{Log}_{10}$ CV | $\text{Log}_{10}$ A | $\text{Log}_{10}$ P95 | TWin | AI   | R2   |
|-----------------|----------------------|---------------------|-----------------------|------|------|------|
| Europe          |                      | 0.03                | 0.04                  | 0.01 | 0.21 | 0.29 |
| Northeastern    |                      | 0.02                | 0.05                  |      | 0.42 | 0.48 |
| Atlantic        |                      | 0.04                |                       | 0.05 | 0.19 | 0.28 |
| Central-Eastern |                      |                     | 0.03                  | 0.14 | 0.44 | 0.61 |
| Alpine          |                      | 0.03                | 0.2                   | 0.01 | 0.13 | 0.37 |
| Mediterranean   |                      | 0.09                | 0.2                   |      | 0.26 | 0.55 |

695

Table A.5: Spearman-Correlation between statistical moments of flood series, including mean specific discharge MAF, mean specific discharge normalized to a catchment area  $\text{MAF}_\alpha$  of  $\alpha=100\text{km}^2$ , the coefficient of variation CV, the coefficient of skewness CS, and catchment attributes. Statistically significant estimates (at the 5% level) are printed in bold.

|       | Europe       |                     |              |              | Northeastern |                     |              |              | Atlantic     |                     |              |              | Central-Eastern |                     |              |              | Alpine       |                     |              |              | Mediterranean |                     |              |              |
|-------|--------------|---------------------|--------------|--------------|--------------|---------------------|--------------|--------------|--------------|---------------------|--------------|--------------|-----------------|---------------------|--------------|--------------|--------------|---------------------|--------------|--------------|---------------|---------------------|--------------|--------------|
|       | MAF          | $\text{MAF}_\alpha$ | CV           | CS           | MAF          | $\text{MAF}_\alpha$ | CV           | CS           | MAF          | $\text{MAF}_\alpha$ | CV           | CS           | MAF             | $\text{MAF}_\alpha$ | CV           | CS           | MAF          | $\text{MAF}_\alpha$ | CV           | CS           | MAF           | $\text{MAF}_\alpha$ | CV           | CS           |
| A     | <b>-0.44</b> | <b>-0.12</b>        | <b>-0.13</b> | <b>-0.13</b> | <b>-0.47</b> | 0.01                | <b>-0.16</b> | <b>-0.07</b> | <b>-0.31</b> | 0.01                | <b>-0.19</b> | <b>-0.08</b> | <b>-0.23</b>    | <b>-0.01</b>        | 0.09         | <b>0.17</b>  | <b>-0.40</b> | 0.02                | <b>-0.03</b> | <b>-0.15</b> | <b>-0.48</b>  | 0.03                | <b>-0.25</b> | <b>-0.18</b> |
| MAP   | <b>0.62</b>  | <b>0.59</b>         | <b>-0.33</b> | <b>-0.01</b> | <b>0.18</b>  | <b>0.15</b>         | <b>-0.23</b> | <b>0.15</b>  | <b>0.64</b>  | <b>0.67</b>         | <b>-0.33</b> | <b>-0.03</b> | <b>0.25</b>     | <b>0.24</b>         | <b>-0.49</b> | <b>-0.38</b> | <b>0.34</b>  | <b>0.26</b>         | <b>-0.61</b> | <b>-0.13</b> | <b>0.42</b>   | <b>0.48</b>         | <b>-0.68</b> | <b>-0.35</b> |
| P95   | <b>0.64</b>  | <b>0.60</b>         | <b>-0.22</b> | 0.02         | <b>0.21</b>  | 0.02                | <b>-0.10</b> | <b>0.17</b>  | <b>0.67</b>  | <b>0.66</b>         | <b>-0.22</b> | 0.00         | <b>0.39</b>     | <b>0.31</b>         | <b>-0.19</b> | <b>-0.26</b> | <b>0.32</b>  | <b>0.24</b>         | <b>-0.58</b> | <b>-0.14</b> | <b>0.49</b>   | <b>0.52</b>         | <b>-0.59</b> | <b>-0.34</b> |
| Pmax  | <b>0.61</b>  | <b>0.55</b>         | <b>-0.05</b> | <b>0.12</b>  | <b>0.19</b>  | <b>-0.04</b>        | <b>-0.09</b> | <b>0.20</b>  | <b>0.53</b>  | <b>0.52</b>         | <b>0.14</b>  | <b>0.17</b>  | <b>0.30</b>     | <b>0.22</b>         | <b>-0.18</b> | <b>-0.23</b> | <b>0.36</b>  | <b>0.26</b>         | <b>-0.40</b> | <b>-0.09</b> | <b>0.57</b>   | <b>0.49</b>         | <b>-0.36</b> | <b>-0.20</b> |
| TSpr  | <b>-0.22</b> | <b>-0.22</b>        | <b>0.26</b>  | 0.00         | <b>-0.31</b> | <b>-0.35</b>        | <b>0.58</b>  | <b>0.23</b>  | <b>-0.29</b> | <b>-0.29</b>        | 0.02         | <b>-0.14</b> | <b>-0.14</b>    | <b>-0.11</b>        | <b>0.50</b>  | <b>0.41</b>  | <b>-0.17</b> | <b>-0.14</b>        | <b>0.38</b>  | <b>-0.04</b> | <b>-0.09</b>  | <b>-0.12</b>        | <b>0.17</b>  | 0.02         |
| TWin  | <b>-0.04</b> | <b>-0.07</b>        | <b>0.04</b>  | <b>-0.06</b> | <b>-0.04</b> | <b>-0.20</b>        | <b>0.20</b>  | <b>0.30</b>  | <b>-0.02</b> | <b>-0.03</b>        | <b>-0.23</b> | <b>-0.17</b> | <b>-0.28</b>    | <b>-0.33</b>        | <b>-0.52</b> | <b>-0.31</b> | <b>-0.11</b> | <b>-0.10</b>        | <b>0.10</b>  | <b>-0.12</b> | <b>0.12</b>   | <b>-0.04</b>        | <b>0.27</b>  | <b>0.14</b>  |
| SM    | <b>0.58</b>  | <b>0.57</b>         | <b>-0.31</b> | <b>-0.03</b> | <b>0.17</b>  | <b>0.16</b>         | <b>-0.14</b> | <b>0.19</b>  | <b>0.52</b>  | <b>0.55</b>         | <b>-0.29</b> | <b>-0.05</b> | <b>0.28</b>     | <b>0.28</b>         | <b>-0.4</b>  | <b>-0.33</b> | <b>0.26</b>  | <b>0.22</b>         | <b>-0.56</b> | <b>-0.10</b> | <b>0.45</b>   | <b>0.50</b>         | <b>-0.64</b> | <b>-0.37</b> |
| PET   | <b>-0.05</b> | <b>-0.03</b>        | <b>0.39</b>  | <b>0.14</b>  | <b>-0.30</b> | <b>-0.33</b>        | <b>0.60</b>  | <b>0.22</b>  | <b>-0.23</b> | <b>-0.22</b>        | <b>0.34</b>  | 0.03         | 0.02            | 0.07                | <b>0.68</b>  | <b>0.45</b>  | <b>-0.16</b> | <b>-0.11</b>        | <b>0.11</b>  | <b>-0.10</b> | <b>-0.11</b>  | <b>-0.21</b>        | <b>0.63</b>  | <b>0.31</b>  |
| AI    | <b>-0.55</b> | <b>-0.53</b>        | <b>0.46</b>  | <b>0.07</b>  | <b>-0.36</b> | <b>-0.36</b>        | <b>0.62</b>  | <b>0.12</b>  | <b>-0.51</b> | <b>-0.53</b>        | <b>0.38</b>  | 0.04         | <b>-0.16</b>    | <b>-0.12</b>        | <b>0.63</b>  | <b>0.50</b>  | <b>-0.39</b> | <b>-0.31</b>        | <b>0.50</b>  | <b>0.08</b>  | <b>-0.37</b>  | <b>-0.43</b>        | <b>0.69</b>  | <b>0.35</b>  |
| Elev  | <b>0.53</b>  | <b>0.55</b>         | <b>0.08</b>  | <b>0.20</b>  | <b>0.35</b>  | <b>0.47</b>         | <b>-0.31</b> | 0.06         | <b>0.38</b>  | <b>0.44</b>         | <b>0.35</b>  | <b>0.22</b>  | <b>0.48</b>     | <b>0.50</b>         | <b>0.21</b>  | <b>0.16</b>  | <b>0.19</b>  | <b>0.16</b>         | <b>-0.47</b> | 0.00         | 0.06          | 0.02                | <b>0.20</b>  | <b>0.20</b>  |
| Slope | <b>0.63</b>  | <b>0.65</b>         | <b>-0.01</b> | <b>0.16</b>  | <b>0.34</b>  | <b>0.39</b>         | <b>-0.36</b> | 0.04         | <b>0.58</b>  | <b>0.62</b>         | <b>0.17</b>  | <b>0.19</b>  | <b>0.29</b>     | <b>0.30</b>         | <b>-0.01</b> | 0.02         | <b>0.25</b>  | <b>0.24</b>         | <b>-0.40</b> | <b>-0.01</b> | <b>0.33</b>   | <b>0.37</b>         | 0.06         | 0.06         |
| LUF   | <b>0.46</b>  | <b>0.45</b>         | <b>-0.10</b> | <b>0.06</b>  | <b>0.30</b>  | <b>0.28</b>         | <b>-0.01</b> | 0.05         | <b>0.43</b>  | <b>0.45</b>         | <b>0.14</b>  | <b>0.14</b>  | 0.08            | 0.01                | <b>-0.39</b> | <b>-0.24</b> | <b>0.27</b>  | <b>0.16</b>         | <b>-0.26</b> | 0.03         | <b>0.40</b>   | <b>0.32</b>         | 0.03         | <b>-0.03</b> |
| LUW   | <b>-0.30</b> | <b>-0.16</b>        | <b>-0.27</b> | <b>-0.15</b> | <b>-0.25</b> | <b>-0.21</b>        | <b>-0.22</b> | <b>-0.06</b> | <b>-0.19</b> | <b>-0.04</b>        | <b>-0.20</b> | <b>-0.06</b> | <b>-0.55</b>    | <b>-0.55</b>        | <b>-0.50</b> | <b>-0.23</b> | <b>-0.16</b> | 0.03                | <b>-0.19</b> | <b>-0.14</b> | <b>-0.40</b>  | <b>-0.10</b>        | <b>-0.19</b> | <b>-0.10</b> |
| Stex  | <b>-0.06</b> | <b>-0.06</b>        | <b>0.29</b>  | <b>0.11</b>  | <b>-0.12</b> | <b>-0.07</b>        | <b>0.37</b>  | <b>0.25</b>  | <b>-0.06</b> | <b>-0.05</b>        | <b>0.17</b>  | <b>-0.01</b> | <b>0.29</b>     | <b>0.32</b>         | <b>0.53</b>  | <b>0.31</b>  | <b>-0.02</b> | <b>-0.06</b>        | <b>0.23</b>  | 0.01         | <b>-0.22</b>  | <b>-0.18</b>        | <b>0.26</b>  | <b>0.16</b>  |

#### Data Availability

The flood data used in this paper are available at [https://github.com/tuwhydro/europe\\_floods](https://github.com/tuwhydro/europe_floods). The authors acknowledge the E-OBS dataset from the EU-FP6 project UERRA (<http://www.uerra.eu>) and the Copernicus Climate Change Service, and the data providers in the ECA&D project (<https://www.ecad.eu>), as well as the CCM River and Catchment database (<https://data.europa.eu>), the Global Aridity Index and Potential Evapo-Transpiration Climate Database (<https://doi.org/10.6084/m9.figshare.7504448.v3>), the CPC Soil Moisture database (<https://www.cpc.ncep.noaa.gov/>), the data on terrain elevation provided by the USGS



705 (<https://www.usgs.gov/>), the Corine Land Cover data set (<https://land.copernicus.eu/>) and the European soil database (<https://esdac.jrc.ec.europa.eu/>).

#### Author Contributions

DL performed the analysis and prepared the paper. GB designed the overall study. All co-authors contributed to the interpretation of the results and writing of the paper.

710

#### Competing Interests

The authors declare that they have no conflict of interest.

#### Acknowledgements

715 The authors would like to acknowledge funding from the Austrian Science Funds (FWF) “SPATE” project I 4776 and the German Research Foundation (DFG; grant no. FOR 2416), the FWF Vienna Doctoral Programme on Water Resource Systems (W1219-N28) and the European Union’s Horizon 2020 Research and Innovation Programme under the Marie Skłodowska-Curie grant agreement no. 676027.

#### 720 References

Amponsah, W. et al. Integrated high-resolution dataset of high-intensity European and Mediterranean flash floods. *Earth Syst. Sci. Data* 10, 1783–1794 (2018).

Azen, R., & Budescu, D. V. (2003). The dominance analysis approach for comparing predictors in multiple regression. *Psychological methods*, 8(2), 129.

725 Bayliss, A. C., & Jones, R. C. (1993). Peaks-over-threshold flood database. Institute of Hydrology.

Berghuijs, W. R., Woods, R. A., Hutton, C. J., & Sivapalan, M. (2016). Dominant flood generating mechanisms across the United States. *Geophysical Research Letters*, 43(9), 4382-4390.

Berghuijs, W. R., Harrigan, S., Molnar, P., Slater, L. J., & Kirchner, J. W. (2019). The relative importance of different flood-generating mechanisms across Europe. *Water Resources Research*, 55(6), 4582-4593.

730 Bertola, M., Viglione, A., Lun, D., Hall, J., & Blöschl, G. (2020). Flood trends in Europe: are changes in small and big floods different?. *Hydrology & Earth System Sciences*, 24(4).

Blöschl, G., & Sivapalan, M. (1995). Scale issues in hydrological modelling: a review. *Hydrological processes*, 9(3-4), 251-290.

735 Blöschl, G. and M. Sivapalan (1997) Process controls on regional flood frequency: Coefficient of variation and basin scale. *Water Resources Research*, 33 (12), pp. 2967-2980.

Blöschl, G., Ardoin-Bardin, S., Bonell, M., Dorninger, M., Goodrich, D., Gutknecht, D., ... & Szolgay, J. (2007). At what scales do climate variability and land cover change impact on flooding and low flows?. *Hydrological Processes*, 21(9), 1241-1247.



- Blöschl, G., Sivapalan, M., Wagener, T., Savenije, H., & Viglione, A. (Eds.). (2013). *Runoff prediction in ungauged basins: synthesis across processes, places and scales*. Cambridge University Press.
- Blöschl, G., Hall, J., Parajka, J., Perdigão, R. A., Merz, B., Arheimer, B., ... & Čanjevac, I. (2017). Changing climate shifts timing of European floods. *Science*, 357(6351), 588-590.
- Blöschl, G., Hall, J., et al. (2019) Changing climate both increases and decreases European river floods. *Nature*, 573(7772), 108-111.
- Blöschl, G., Kiss, A., Viglione, A. et al. Current European flood-rich period exceptional compared with past 500 years. *Nature* 583, 560–566 (2020). <https://doi.org/10.1038/s41586-020-2478-3>
- Boorman, D. B., Hollis, J. M., & Lilly, A. (1995). *Hydrology of soil types: a hydrologically-based classification of the soils of United Kingdom*. Institute of Hydrology
- Brath, A., Montanari, A., & Moretti, G. (2006). Assessing the effect on flood frequency of land use change via hydrological simulation (with uncertainty). *Journal of Hydrology*, 324(1-4), 141-153.
- Cornes, R. C., van der Schrier, G., van den Besselaar, E. J., & Jones, P. D. (2018). An ensemble version of the E-OBS temperature and precipitation data sets. *Journal of Geophysical Research: Atmospheres*, 123(17), 9391-9409.
- Cressie, N. A. (1993). *Statistics for spatial data*. John Wiley and Sons. Inc., New York.
- Fan, Y., & Van Den Dool, H. (2004). Climate Prediction Center global monthly soil moisture data set at 0.5 resolution for 1948 to present. *Journal of Geophysical Research: Atmospheres*, 109(D10).
- Farquharson, F. A. K., Meigh, J. R., & Sutcliffe, J. V. (1992). Regional flood frequency analysis in arid and semi-arid areas. *Journal of Hydrology*, 138(3-4), 487-501.
- Gaál, L., J. Szolgay, S. Kohnová, J. Parajka, R. Merz, A. Viglione and G. Blöschl (2012) Flood timescales: Understanding the interplay of climate and catchment processes through comparative hydrology, *Water Resources Research*, 48, W04511, doi:10.1029/2011WR011509.
- Gaume, E., V. Bain, P. Bernardara, O. Newinger, M. Barbuc, A. Bateman, L. Blaškovicová, G. Blöschl, M. Borga, A. Dumitrescu, I. Daliakopoulos, J. Garcia, A. Irimescu, S. Kohnova, A. Koutroulis, L. Marchi, S. Matreata, V. Medina, E. Preciso, D. Sempere-Torres, G. Stancalie, J. Szolgay, I. Tsanis, D. Velasco and A. Viglione (2009) A compilation of data on European flash floods. *Journal of Hydrology*, 367 (1-2), 70-78.
- Gibbons, J. D. and Chakraborti, S. (2010) *Nonparametric Statistical Inference*. CRC Press, Boca Raton 650pp.
- Gioia, A., Iacobellis, V., Manfreda, S., & Fiorentino, M. (2012). Influence of infiltration and soil storage capacity on the skewness of the annual maximum flood peaks in a theoretically derived distribution. *Hydrology and Earth System Sciences*, 16(3), 937.
- Giorgi, F., Bi, X., & Pal, J. S. (2004). Mean, interannual variability and trends in a regional climate change experiment over Europe. I. Present-day climate (1961–1990). *Climate Dynamics*, 22(6), 733-756.



- 775 Grillakis, M.G., A.G. Koutroulis, J. Komma, I.K. Tsanis, W. Wagner, G. Blöschl (2016) Initial soil moisture effects on flash flood generation – A comparison between basins of contrasting hydro-climatic conditions. *Journal of Hydrology*, Volume 541, Part A, 206–217.
- Hall, J., Arheimer, B., Aronica, G. T., Bilibashi, A., Bohác, M., Bonacci, O., ... & Claps, P. (2015). A European Flood Database: facilitating comprehensive flood research beyond administrative boundaries. *Changes in Flood Risk and Perception in Catchments and Cities*, 370, 89-95.
- 780 Hall, J. and G. Blöschl (2018) Spatial patterns and characteristics of flood seasonality in Europe, *Hydrology and Earth System Sciences*, 22, pp. 3883-3901, <https://doi.org/10.5194/hess-22-3883-2018>
- Hofstätter M., Lexer A., Homan M. and G. Blöschl (2018) Large-scale heavy precipitation over central Europe and the role of atmospheric cyclone track types. *International Journal of Climatology*, 38, pp. e497–e517, <https://doi.org/10.1002/joc.5386>
- 785 Hofstätter, M., & Blöschl, G. (2019). Vb cyclones synchronized with the Arctic-/North Atlantic Oscillation. *Journal of Geophysical Research: Atmospheres*, 124(6), 3259-3278.
- Iacobellis, V., Claps, P., and Fiorentino, M.: Climatic control on the variability of flood distribution, *Hydrol. Earth Syst. Sci.*, 6, 229–238, <https://doi.org/10.5194/hess-6-229-2002>, 2002.
- Kendall, M. & Stuart, A. (1969). *The advanced theory of statistics*. London: Griffin.
- 790 Lilly, A., Boorman, D. B., & Hollis, J. M. (1998). The development of a hydrological classification of UK soils and the inherent scale changes. In *Soil and Water Quality at Different Scales* (pp. 299-302). Springer, Dordrecht.
- Marchi, L., M. Borgia, E. Preciso, and E. Gaume (2010), Characterisation of selected extreme flash floods in Europe and implications for flood risk management, *Journal of Hydrology*, 394(1–2), 118–133, doi:10.1016/j.jhydrol.2010.07.017.
- 795 Maréchal, D., & Holman, I. P. (2005). Development and application of a soil classification-based conceptual catchment-scale hydrological model. *Journal of Hydrology*, 312(1-4), 277-293.
- Merz R. and G. Blöschl (2003) A process typology of regional floods. *Water Resources Research*, 39 (12), article number 1340.
- 800 Merz, R., Blöschl, G., & Parajka, J. (2006). Spatio-temporal variability of event runoff coefficients. *Journal of Hydrology*, 331(3-4), 591-604.
- Merz, R., & Blöschl, G. (2008a). Flood frequency hydrology: 1. Temporal, spatial, and causal expansion of information. *Water Resources Research*, 44(8).
- Merz, R., & Blöschl, G. (2008b). Flood frequency hydrology: 2. Combining data evidence. *Water Resources Research*, 44(8).
- 805 Merz R and G. Blöschl (2009) Process controls on the statistical flood moments - a data based analysis. *Hydrological Processes*, 23 (5) 675-696.



- Miller, J. D., & Brewer, T. (2018). Refining flood estimation in urbanized catchments using landscape metrics. *Landscape and Urban Planning*, 175, 34-49.
- 810 Mimikou, M., & Gordios, J. (1989). Predicting the mean annual flood and flood quantiles for ungauged catchments in Greece. *Hydrological sciences journal*, 34(2), 169-184.
- Pallard, B., Castellarin, A., and Montanari, A.: A look at the links between drainage density and flood statistics, *Hydrol. Earth Syst. Sci.*, 13, 1019–1029, <https://doi.org/10.5194/hess-13-1019-2009>, 2009.
- Panagos P., Van Liedekerke M., Jones A., Montanarella L., “European Soil Data Centre: Response to European policy support and public data requirements”; (2012) *Land Use Policy*, 29 (2), pp. 329-338.  
815 doi:10.1016/j.landusepol.2011.07.003
- Penna, D., Tromp-van Meerveld, H. J., Gobbi, A., Borga, M., & Dalla Fontana, G. (2011). The influence of soil moisture on threshold runoff generation processes in an alpine headwater catchment. *Hydrology and Earth System Sciences*, 15(3), 689-702.
- Perdigão, R. A. P., and G. Blöschl (2014) Spatiotemporal flood sensitivity to annual precipitation: Evidence for  
820 landscape-climate coevolution, *Water Resour. Res.*, 50, 5492-5509, doi:10.1002/2014WR015365.
- Peschke, G., & Sambale, C. (1999). Hydrometric approaches to gain a better understanding of saturation excess overland flow. *IAHS PUBLICATION*, 13-22.
- Picciafuoco, T., R. Morbidelli, A. Flammini, C. Saltalippi, C. Corradini, P. Strauss and G. Blöschl (2019) A  
825 pedotransfer function for field-scale saturated hydraulic conductivity of a small watershed. *Vadose Zone Journal* 18, 190018. doi:10.2136/vzj2019.02.0018
- Roekaerts, M. (2002) The biogeographical regions map of Europe. Basic principles of its creation and overview of its development. Copenhagen: European Environment Agency. <https://www.eea.europa.eu/data-and-maps/data/biogeographical-regions-europe-3>
- Rogger, M., H. Pirkel, A. Viglione, J. Komma, B. Kohl, R. Kirnbauer, R. Merz, and G. Blöschl (2012), Step  
830 changes in the flood frequency curve: Process controls, *Water Resour. Res.*, 48, W05544, doi:10.1029/2011WR011187.
- Rogger, M., Viglione, A., Derx, J., & Blöschl, G. (2013). Quantifying effects of catchments storage thresholds on step changes in the flood frequency curve. *Water Resources Research*, 49(10), 6946-6958.
- Rogger, M., M. Agnoletti, A. Alaoui, J.C. Bathurst., G. Bodner, M. Borga, V. Chaplot, F. Gallart, G. Glatzel, J.  
835 Hall, J. Holden, L. Holko, R. Horn, A. Kiss, S. Kohnova, G. Leitinger, B. Lennartz, J. Parajka, R. Perdigão, S. Peth, L. Plavcová, J.N. Quinton, M. Robinson, J.L. Salinas, A. Santoro, J. Szolgay, S. Tron, J.J.H. van den Akker, A. Viglione and G. Blöschl (2017) Land-use change impacts on floods at the catchment scale: Challenges and opportunities for future research. *Water Resources Research*, 53, 5209–5219, doi:10.1002/2017WR020723.
- 840 Rosbjerg, D., G. Blöschl, D. H. Burn, A. Castellarin, B. Croke, G. DiBaldassarre, V. Iacobellis, T. R. Kjeldsen, G. Kuczera, R. Merz, A. Montanari, D. Morris, T. B. M. J. Ouarda, L. Ren, M. Rogger, J. L. Salinas, E. Toth, A. Viglione (2013) Prediction of floods in ungauged basins. Chapter 9 in: G. Blöschl, M.





- 845 Sivapalan, T. Wagener, A. Viglione, H. Savenije (Eds.) Runoff Prediction in Ungauged Basins -  
Synthesis across Processes, Places and Scales. Cambridge University Press, Cambridge, UK, pp. 135-  
162.
- Salinas, J. L., Castellarin, A., Viglione, A., Kohnova, S., & Kjeldsen, T. R. (2014a). Regional parent flood  
frequency distributions in Europe-Part 1: Is the GEV model suitable as a pan-European  
parent?. *Hydrology and Earth System Sciences*, 18(11), 4381.
- Salinas, J. L., Castellarin, A., Kohnova, S., & Kjeldsen, T. R. (2014b). Regional parent flood frequency  
850 distributions in Europe-Part 2: Climate and scale controls. *Hydrol. Earth Syst. Sci.*, 18(11), 4391-4401.
- Schmocker-Fackel, P., Näf, F., & Scherrer, S. (2007). Identifying runoff processes on the plot and catchment  
scale. *Hydrology and Earth System Sciences*, 11(2), 891-906.
- Scherrer, S., Naef, F., Faeh, A. O., & Cordery, I. (2007). Formation of runoff at the hillslope scale during intense  
precipitation. *Hydrology and Earth System Sciences*, 11(2), 907-922.
- 855 Sivapalan, M. (2003) Process complexity at hillslope scale, process simplicity at the watershed scale: is there a  
connection? *Hydrol. Process.*, 17 (5) (2003), pp. 1037-1041
- Sivapalan, M., Blöschl, G., Merz, R., & Gutknecht, D. (2005). Linking flood frequency to long-term water  
balance: Incorporating effects of seasonality. *Water Resources Research*, 41(6).
- Smith, J. A. (1992). Representation of basin scale in flood peak distributions. *Water Resources Research*, 28(11),  
860 2993-2999.
- Šraj, M., Viglione, A., Parajka, J., & Blöschl, G. (2016). The influence of non-stationarity in extreme  
hydrological events on flood frequency estimation, *Journal of Hydrology and Hydromechanics*, 64(4),  
426-437. doi: <https://doi.org/10.1515/johh-2016-0032>
- Sun, D., Yang, H., Guan, D., Yang, M., Wu, J., Yuan, F., ... & Zhang, Y. (2018). The effects of land use change  
865 on soil infiltration capacity in China: A meta-analysis. *Science of the Total Environment*, 626, 1394-  
1401.
- Trabucco, A., & Zomer, R. J. (2018). Global aridity index and potential evapotranspiration (ET<sub>0</sub>) climate  
database v2. CGIAR Consortium for Spatial Information (CGIAR-CSI). Available online:  
[https://figshare.  
870 com/articles/Global\\_Aridity\\_Index\\_and\\_Potential\\_Evapotranspiration\\_ET0\\_Climate\\_Database\\_v2/750  
4448/1](https://figshare.com/articles/Global_Aridity_Index_and_Potential_Evapotranspiration_ET0_Climate_Database_v2/7504448/1) (accessed on 25 June 2019).
- Troch, P. A., T. Lahmers, A. Meira, R. Mukherjee, J. W. Pedersen, T. Roy, and R. Valdés-Pineda (2015). Catchment coevolution: A useful framework for improving predictions of hydrological change?.  
*Water Resour. Res.*, 51, 4903–4922, doi:10.1002/2015WR017032.
- 875 Viglione, A., R. Merz and G. Blöschl (2009) On the role of the runoff coefficient in the mapping of rainfall to  
flood return periods, *Hydrology and Earth System Sciences*, 13 (5) 577 - 593.



- Viglione, A., G. B. Chirico, R. Woods and G. Blöschl (2010a) Generalised synthesis of space–time variability in flood response: An analytical framework. *Journal of Hydrology*, 394 (1–2), 198–212.  
doi:10.1016/j.jhydrol.2010.05.047.
- 880 Viglione, A., Chirico, G. B., Komma, J., Woods, R., Borga, M., & Blöschl, G. (2010b). Quantifying space-time dynamics of flood event types. *Journal of Hydrology*, 394(1-2), 213-229. (not sure if this is the right citation, appears in text)
- Viglione, A., Merz, R., Salinas, J. L., & Blöschl, G. (2013). Flood frequency hydrology: 3. A Bayesian analysis. *Water Resources Research*, 49(2), 675-692.
- 885 Viglione, A., Merz, B., Viet Dung, N., Parajka, J., Nester, T., & Blöschl, G. (2016). Attribution of regional flood changes based on scaling fingerprints. *Water resources research*, 52(7), 5322-5340.
- Vogt, J., Soille, P., De Jager, A., Rimaviciute, E., Mehl, W., Foisneau, S., Bodis, K., Dusart, J., Paracchini, M., Haastrup, P., et al.: A pan-European river and catchment database, European Commission, EUR, 22920, 120, 2007.
- 890 Wang, W., H.-Y. Li, L. R. Leung, W. Yigzaw, J. Zhao, H. Lu, Z. Deng, Y. Demisie and G. Blöschl (2017) Nonlinear filtering effects of reservoirs on flood frequency curves at the regional scale. *Water Resources Research*, 53, 8277–8292, doi: 10.1002/2017WR020871
- Weingartner, R., Barben, M., & Spreafico, M. (2003). Floods in mountain areas—an overview based on examples from Switzerland. *Journal of Hydrology*, 282(1-4), 10-24.
- 895 Weisberg, S. (2005) *Applied linear regression*. John Wiley & Sons, Hoboken, NJ, 352 pp.
- Xoplaki, E., Gonzalez-Rouco, J. F., Luterbacher, J. & Wanner, H. Wet season Mediterranean precipitation variability: influence of large-scale dynamics and trends. *Clim. Dyn.* 23, 63–78 (2004).
- Zaman, M. A., Rahman, A., & Haddad, K. (2012). Regional flood frequency analysis in arid regions: A case study for Australia. *Journal of Hydrology*, 475, 74-83.